C.P. No. 753

C.P. No. 753

MINISTRY OF AVIATION

AERONAUTICAL RESEARCH COUNCIL

CURRENT PAPERS

Wind Tunnel Tests at M=2.0 on Interference Effects between Intake Flows in a Four-Engine Nacelle

by

M. D. Dobson

LONDON: HER MAJESTY'S STATIONERY OFFICE

1964

TEN SHILLINGS NET

U.D.C. No. 533.697.2 : 533.6.011.5 : 533.695.9 : 621.438.018

C.P. No. 753

September, 1963

WIND TUNNEL TESTS AT M = 2.0 ON INTERFERENCE EFFECTS BETWEEN INTAKE FLOWS IN A FOUR-ENGINE NACELLE

by

M. D. Dobson

SUMMARY

A model of a rectangular air intake of aspect ratio 8, with all-external compression and a fixed geometry, has been tested at its design Mach number of 2.0 in the 3 ft × 3 ft wind tunnel. The model contained four side-by-side simulated engine cells and tests were made to investigate effects on pressure recovery and mass flow in each of the cells for conditions of unequal throttling.

Results showed that when the throttle of one cell was closed to give sub-critical inlet flow, the shock geometry at the inlet was affected and pressure recovery and mass flow in the remaining cells were reduced. These reductions became progressively smaller in cells situated further from the throttle cell. Both pressure recovery and mass flow in a cell adjacent to one which was passing reduced flow were affected also by the presence of duct dividers in the intake.

When the throttle of one cell was opened to give super-critical inlet flow, an adjacent cell was not affected if the duct was divided between the cells from the beginning of the subsonic diffuser. If the cells shared a common diffuser the adjacent cell suffered reductions in both pressure recovery and mass flow.

Schlieren observations indicate that the initial onset of instability under sub-critical flow conditions, occurs at the same mean mass flow ratio, irrespective of how the four throttles are individually set to achieve this ratio.

Replaces R.A.E. Tech Note No. Aero 2920 - A.R.C. 25,597.

CONTENTS

		Page
1	INTRODUCTION	5
2	EXPERIMENTAL DETAILS	5
	2.1 Model	5
	2.2 Instrumentation	6
	2.3 Scope of tests	6
3	RESULTS	7
	3.1 Reduction and presentation	7
	3.2 Cells throttled in unison	7
	3.3 Cells throttled unequally	8
	3.4 Intake stability	11
4	FURTHER WORK	12
5	CONCLUSIONS	12
REFERENCES		13

ILLUSTRATIONS - Figs.1-27

DETACHABLE ABSTRACT CARDS

ILLUSTRATIONS

	Fig.
Outline drawing of model	1
Photographs of model	2
Variation of pressure recovery with mass flow ratio, configuration A, four cells throttled together	3
Variation of pressure recovery with mass flow ratio, configuration B, four cells throttled together	4
Schlieren photographs, configuration A, with all four cells throttled together	5
Sketches of shock configurations showing how variation of $\bar{H}/H_\infty$ with A_∞/A_{en} is achieved	6
Total pressure distributions looking downstream, configuration A	7

ILLUSTRATIONS (CONTD)

	Fig.
Total pressure distributions looking downstream, configuration B	8
Variation of pressure recovery with mass flow ratio, configuration A, cell 1 throttled	9
Variation of pressure recovery with mass flow ratio, configuration A, cell 2 throttled	10
Block diagrams showing pressure recovery and spillage in cells when cell 1 is throttled, configuration A	11
Block diagrams showing pressure recovery and spillage in cells when cell 2 is throttled, configuration A	12
Schlieren photograph, configuration A, cell 1 throttled to $A_\infty/A_{en} \simeq 0.43$	13
Sketch showing asymmetric normal shock front when cell 1 is throttled	14
Variation of pressure recovery with mass flow ratio, configuration B, cell 1 throttled	15
Variation of pressure recovery with mass flow ratio, configuration B, cell 2 throttled	16
Block diagrams showing pressure recovery and spillage in cells when cell 1 is throttled, configuration B	17
Block diagrams showing pressure recovery and spillage in cells when cell 2 is throttled, configuration B	18
$\frac{Q_I}{Q_T}$ - variation with spillage from throttled cell	19
Variation across the inlet span of the relative positions of the intersections of the oblique and normal shocks and the limiting entry streamline and normal shock	20
Shock configurations for the case of "adjacent" cell having lower mean pressure recovery than "throttled" cell	21
Total pressure distributions looking downstream, cell 1 throttled to $A_c/A_{en} \simeq 0.43$	22
Variation of pressure recovery with mass flow ratio, configuration A, cells 1 and 2 throttled	23

ILLUSTRATIONS (CONTD)

	Fig.
Block diagrams showing pressure recovery and spillage in cells when cells 1 and 2 are throttled, configuration A	24
Variation of pressure recovery with mass flow ratio, configuration B, cells 1 and 2 throttled	25
Block diagrams showing pressure recovery and spillage in cells when cells 1 and 2 are throttled, configuration B	26
Schlieren photographs showing intake instability, configuration A	27

1 INTRODUCTION

A type of engine installation which has come under consideration for supersonic aircraft consists of partially buried engines contained in rectangular nacelles, with ramp-compression intakes. The nacelles contain engines situated side-by-side and it is important to know the nature and extent of interference effects which may exist between the flows to different engines, if for any reason the latter are not all functioning identically.

To investigate some initial aspects of this problem a generalised model of a typical nacelle containing four side-by-side simulated engines has been made and tested in the 3 ft × 3 ft tunnel. The model had an all-external compression intake with a single 14° ramp and was designed for the oblique shock wave to fall on the lip at M = 2.0. The intake geometry was assumed to be fixed, the tests being thereby restricted to simulating the effects of variations in engine and nozzle conditions.

2 EXPERIMENTAL DETAILS

2.1 Model

An outline drawing of the model is shown in Fig.1 and photographs in Fig.2. The inlet lip was at a height of 2 inches above the datum and the inlet was 16 inches wide, thus the aspect ratio* was 8 and maximum entry stream tube area was 32 sq inches. The throat area was 0.95 of the inlet area (inlet height in this case measured normal to the ramp surface); this contraction occurred partly because of the presence of a wedge forming the leading edge of a central web (see Fig.1 and next paragraph). Downstream of the contraction the area of the duct remained constant for a distance of about $2\frac{1}{2}$ throat heights (region A, Fig.1), after which the subsonic diffuser (region B) began. The area distribution along the diffuser was equal to that of a cone with a 6° vertex angle and the final area was 1.05 times the area of the simulated compressor annuli. Downstream of the diffuser was a transition section (region C) which arbitrarily faired the rectangular duct into the four individual cells which simulated the engines. The ducting through each cell remained constant in area and each cell incorporated means of controlling the flow and measuring it.

The main duct was divided longitudinally by a central web which was necessary to prevent distortion of the model, especially at the lip**. This central web extended from the inlet plane (see Fig.1) downstream to the cells. Provision was also made for the duct to be split into four by the insertion of a pair of "splitter" plates which extended from the beginning of the subsonic diffuser (see Fig.1) downstream to the cells.

---

* Aspect ratio for the intake is defined as:-

$$\frac{\text{inlet width}}{\text{height of lip above ramp leading-edge}}$$

** This central web might also be necessary at full scale.

The model was mounted on the tunnel floor and raised well clear of the tunnel boundary layer on vanted I-section beams.

2.2 Instrumentation

The instrumentation contained in each cell consisted of twelve pitot pressure tubes and four static pressure holes. The pitot tubes were mounted on a rotatable rake, across a diameter, with six tubes on each arm. They were positioned radially at centres of area of six annuli of equal area. The four pitot rakes (one in each cell) were mechanically linked so that they rotated in unison. Static pressure holes in each cell were located in the outer walls of the ducts at angular positions of 0°, 90°, 180° and 270°.

Mass flow through each cell was controlled by a conical throttle and the four throttles could be actuated together or disconnected individually and locked in any position. Thus, for example, three cells could have their throttles set to pass the full entry stream tube while the fourth was moved to pass a smaller flow.

2.3 Scope of tests

The configurations which were tested are designated as follows:-

Configuration A Model with central longitudinal web.

Configuration B As configuration A but with "splitter" plates.

The method of test for each configuration was initially to throttle all four cells together and make pressure surveys at various values of mass flow. During these tests, the position of the throttles was noted for which the inlet flow became critical, i.e. the point at which the normal shock lies in the inlet plane. Having established this position further tests were made in which:-

(a) cells 2, 3 and 4 had their throttles set in this position while the throttle of cell 1 (port outer) was moved,

(b) cells 1, 3 and 4 set while the throttle of cell 2 (port inner) was moved,

and (c) cells 3 and 4 set while the throttle of cells 1 and 2 were moved together.

Pressure surveys were made in some cases by taking readings at rake rotation angles of $0^{\circ} \times 15^{\circ}$ to 165° and in other cases by taking readings at 0° and 90° only. The former are referred to as comprehensive surveys and the latter as limited surveys.

Pressure measurements were confined to stable inlet flow conditions which were ensured by observation of the schlieren image. There were however isolated instances of shock oscillation over small ranges of mass flow within the test mass flow range. No measurements were made of fluctuating pressure within the ducting; this will be the subject of further tests.

To fix transition of the boundary layer at the inlet, a band of distributed roughness was applied to the ramp surface, sidewalls and central web. This band

was about 0.25 inch wide and was positioned about 0.25 inch from the leading edge in each case. The roughness consisted of 100 grade carborundum grains (maximum height 0.007 inch) secured to the model with aluminium paint.

The test Mach number was 2.00 and the Reynolds number 0.12×10^6 per inch.

3 RESULTS

3.1 Reduction and presentation

Pressure recovery, $\bar{H}/H_{\infty}$, is the measuring-station mean total pressure, (mass flow weighted), compared with free stream total pressure. Mass flow ratio, A_{∞}/A_{en} is quoted as the entry stream tube area compared with the entry area. In the calculations the values of pressure (and hence velocity) measured by the outer and inner pitot tubes on each arm of a rake are assumed to extend to the surfaces of the wall and central hub respectively in each cell. Thus no allowance has been made for the boundary layers on these surfaces. In some cases, other than where the result might be expected (see section 3.3), experimental values of A_{∞}/A_{en} are found to be greater than unity and it is thought that neglect of the boundary layer in the calculation of mass flow may account for this. The values of mean pressure recovery also may be slightly optimistic for the same reason but it is considered that any errors are less than 0.005.

Throughout the results, on curves of pressure recovery plotted against mass flow, circular symbols indicate experimental points which were obtained from comprehensive pressure surveys and triangular symbols, points which were obtained from limited pressure surveys. It is interesting to note how well these align with each other. Arrows on these curves, for cells whose throttles are fixed, indicate the order of experimental points in the direction of opening the throttle(s) of the other cell(s).

3.2 Cells throttled in unison

The variation of pressure recovery with mass flow ratio for the case in which all four cells are throttled together, is shown in Figs.3 and 4 for configurations A and B respectively. A series of schlieren photographs taken at various values of mass flow ratio for configuration A are shown in Fig.5. It will be noted that in Figs.5(d), (e) and (h) the shock system at the inlet is unsteady. The corresponding values of mass flow ratio are 0.85, 0.78 and 0.62 respectively and thus no experimental points appear at these values on the pressure recovery characteristics. These local instabilities were also found to be present at similar values of A_{∞}/A_{en} with configuration B.

Comparing Figs.3 and 4, corresponding curves for the two configurations are similar and in each case the curves for the four cells are similar except that the outer two cells appear to accept a maximum mass flow 4% - 5% greater than the inner two; the reason for this is not clear. A peak pressure recovery of about 0.85 is attained in each cell when the inlet flow is critical, as sketched in Fig.6(a), and this compares with a theoretical maximum value of 0.896 calculated from the recovery through the oblique and normal shock waves. It is worth noting that tests[1] on a single cell intake with a 14° compression ramp and a similar diffuser also produced a maximum recovery of about 0.85 at M = 2.0.

As the cells are throttled the schlieren photographs indicate that the shock system at the inlet is gradually expelled and Figs.3 and 4 show that both mass flow ratio and pressure recovery fall steadily, at similar rates in each cell.

At a mass flow ratio of between 0.45 and 0.50 (slight variation between cells), pressure recovery reaches a value of approximately 0.715 and ceases to fall with further decrease in mass flow. The schlieren photograph (Fig.5(i)) taken at a mass flow ratio of 0.56 indicates that the intake normal shock has been expelled to the vicinity of the ramp leading edge. As this condition is approached the shock pattern sketched in Fig.6(b) exists, in which virtually all the entering stream tube passes through a single shock. Over the area of the stream tube this shock is nearly normal and thus the theoretical pressure recovery through it is approximately 0.72. Figs.5(j) and (k) are schlieren photographs taken at lower values of mass flow ratio and show a detached normal shock ahead of the ramp which gives a similar theoretical pressure recovery. Figs.5(e), (f) and (g) are schlieren photographs taken at intermediate values of mass flow and in Fig.6(c) is sketched a typical shock pattern for such values. Here part of the entering flow passes through a single normal shock and part through both the oblique and normal shocks, thus the pressure recovery lies between the theoretical minimum and maximum values of 0.721 and 0.896.

Total pressure distributions at the measuring stations are given for configuration A in Fig.7. Fig.7(a) shows the case for all cells throttled equally to a mass flow ratio of approximately 0.72 and Fig.7(b) for all four throttles set to give critical inlet flow. Fig.8 shows similar cases for configuration B except that in Fig.8(a) the mass flow ratio is approximately 0.66. The isobars show lines of constant pressure recovery. When the inlet flow is critical, fairly severe pressure gradients exist across the faces of the cells for both configurations and maximum differences of 0.12 H_∞ are noted. The pressure gradients are mainly radial and are indicative of the boundary layer on the dividing walls in the diffuser. Thus gradients are noticeably absent between cells 1 and 2 and between cells 3 and 4 for configuration A, i.e. when there is no dividing wall. In each case, when the cells are throttled to the lower value of mass flow ratio, the isobars remain similar in shape but the severity of the pressure gradients is reduced. In all cases the isobar pattern is roughly symmetrical about a horizontal datum.

3.3 Cells throttled unequally

Curves of pressure recovery against mass flow ratio for configuration A, in the case with one cell being throttled while the throttles of the other three cells are set in the critical inlet flow position, are shown in Figs.9 and 10. Fig.9 shows results for cell 1 being throttled and Fig.10 for cell 2 being throttled. In both cases when the throttled cell is passing reduced flow the mass flow and pressure recovery in the other three cells are reduced. The magnitude of these reductions appears to vary in each cell with its proximity to the throttled cell, i.e. the closer to the throttled cell the larger the reductions.

The effects of throttling cell 1 and cell 2 are illustrated in Figs.11 and 12 respectively, by means of block diagrams. These show the spillage $(1-A_\infty/A_{en})$, in each cell, together with corresponding pressure recoveries, for

spillage values in the throttled cell of approximately 0.57, 0.21 and 0.09. The total quantity of air spilled from the intake appears to be independent of which cell is throttled and is approximately 1.5 times the quantity of air spilled from the throttled cell.

At a spillage value of 0.57, the pressure recovery in the throttled cell, (approximately 0.75 in cell 1 and 0.78 in cell 2), is greater than might have been expected from the results shown in Fig. 3 where, when all four cells were throttled to this value of spillage, the average pressure recovery was at the minimum value of 0.715. The relatively high values suggest that there exists a combination of inclined and normal shocks in front of the whole inlet and this is well illustrated by comparing the schlieren photographs of Figs.5(j) and (k) with Fig.13. As may be seen a certain amount of the flow in the latter case is still passing through the two shock system. Thus the normal shock in front of the cell passing reduced mass flow is not expelled as far as would be expected from the flow passing through that cell. This may be of significance from the point of view of intake stability, particularly with regard to intakes having a limited sub-critical stable mass flow range.

In the case of one cell in a bank of four being throttled, it seems likely that the normal shock is expelled not only immediately upstream of the throttled cell but in an asymmetric manner over the whole inlet, thus affecting the un-throttled cells. This condition is shown diagrammatically in Fig.14; it would explain the reductions in mass flow ratio and pressure recovery noted and the way in which the magnitude of these reductions varies across the intake.

Pressure characteristics for configuration B with cell 1 throttled and again with cell 2 throttled are shown in Figs.15 and 16 respectively and corresponding block diagrams are given in Figs.17 and 18.

Fig.19 shows the ratio:-

$$\frac{\text{total quantity of air spilled from the intake}}{\text{quantity of air spilled from the throttled cell}}$$ plotted

against $(1 - A_\infty/A_{en})$ for the throttled cell. It will be seen that this ratio is always greater for configuration B than configuration A.

The following table shows the spillage from a cell adjacent to the throttled cell, (taken from Figs.11, 12, 17 and 18), with reference to the type of division of the ducting upstream. The values are for 0.57 spillage from the throttled cell.

	Type of division of ducting between throttled and adjacent cell		
	No division	Central web (type-A division)	Splitter plate (type-B division)
Values of $(1 - A_\infty/A_{en})$	0.130 0.120	0.085 0.105	0.190 0.185
Average	0.125	0.095	0.187

It should be remembered that of these values, some are for an outer cell and some for an inner cell; the differences between these cases, however, appear to be small. From the table it appears that relative to no division of the ducting, the mass flow ratio through an adjacent cell is improved by 0.03 if the duct has a type-A division but reduced by approximately 0.06 if the duct has a type-B division.

In general the lowest mean pressure recovery is recorded not in the throttled cell but in one adjacent to it (see Figs.12, 17 and 18). One simple explanation of this could be as follows. The position forward of the normal shock from the entry plane across the inlet span is now not directly proportional to the flow spillage from any particular cell as it is when all four cells are throttled together. Thus although the normal shock may be nearer the entry plane ahead of an adjacent cell, in fact a larger proportion of the flow may be going through the single shock, rather than the two shock system, than is the case for the throttled cell itself. The point is illustrated in Figs. 20 and 21. The relative variations of limiting entry streamline position and shock intersection height are probably altered by the spanwise position of the cell being throttled. It is thought that these may also be affected by the streamwise extent of the dividing walls between the cells; thus comparison of Figs.11 and 12 with Figs.17 and 18 shows that lower pressure recoveries are recorded in "adjacent" cells separated from the throttled cell by type-B division, than in those separated by type-A division. These differences in pressure recovery are also illustrated in Fig.22 which shows total pressure distributions for configurations A and B with cell 1 throttled to $A_\infty/A_{en} \simeq 0.43$ in each case.

From the point of view of interference between adjacent cells when one is throttled, it therefore appears to be detrimental to divide the duct with a splitter plate which extends from the beginning of the subsonic diffuser, since the adjacent cell suffers greater reductions in both mass flow ratio and pressure recovery than it would if the duct were not divided. However, if the duct is divided from the inlet plane, small increases are obtained in mass flow and pressure recovery in the adjacent cell.

If the throttle of cell 1 is opened beyond the position for critical inlet flow, Fig.9 shows that for configuration A the mass flow ratio in cell 1 continues to increase to values greater than 1.0, though its pressure recovery falls. Both pressure recovery and mass flow ratio in cell 2 are seen to fall appreciably but apart from a slight reduction in mass flow ratio, cells 3 and 4 remain unaffected. Under similar conditions of throttle opening with configuration B (Fig.15), mass flow ratio is seen not to increase beyond its normal value in cell 1 and the pressure recoveries in cells 2, 3 and 4 are unaffected. Thus if two cells are served by a common subsonic diffuser and the throttle of one is opened to give super-critical inlet flow, cross flow occurs in the diffuser resulting in increased mass flow through this cell at the expense of both mass flow and pressure recovery in the adjacent cell. This is prevented if each cell has a separate diffuser.

Pressure characteristics and block diagrams for the case in which cells 3 and 4 are set to the critical inlet flow position while cells 1 and 2 are throttled together, are shown for configurations A and B in Figs.23 and 24

and 25 and 26 respectively. These results show little difference between the two configurations and interference effects are as would be expected from consideration of the cases with one cell only being throttled.

3.4 Intake stability

Although no measurements of pressure fluctuations within the ducting were made, study of schlieren photographs affords some qualitative indication of the stability characteristics of the intake. All the schlieren photographs discussed were taken with model configuration A.

Fig.5 presents a series of photographs taken over a range of mass flow ratio from 1.0 to 0.39 for the case in which all four cells were throttled together. Two regions of instability are shown, the first at $A_\infty/A_{en} \simeq 0.85$ to 0.78 and the second at $A_\infty/A_{en} \simeq 0.62$. The flow becomes stable at mass flows between these two regions and again below $A_\infty/A_{en} \simeq 0.62$.

When one cell or two cells together were throttled, only one unstable region was encountered in each case. Schlieren photographs are shown in Fig. 27. Also included in this Fig. are photographs of the first sub-critical unstable region encountered when all four cells were throttled together. In each case of throttling, the upper photograph shows stable sub-critical flow, the centre photograph unstable flow and the lower photograph the flow becoming stable again at lower values of A_∞/A_{en}.

Fig.27 (b), (e) and (h) indicates that the first sub-critical region of unstable flow occurs, in each case of throttling, at a mean mass flow ratio (the mean of the mass flow ratios measured in the four cells) of about 0.85. The following table shows the approximate mass flow ratio in each of the cells at the point of onset of instability:-

Cells throttled	Mass flow ratios in:- Cell 1	Cell 2	Cell 3	Cell 4	Mean A_∞/A_{en}
1	0.61	0.91	0.92	0.97	0.85
1 and 2	0.73	0.73	0.94	0.95	0.84
1, 2, 3 and 4	0.86	0.83	0.86	0.86	0.85

It therefore may be concluded that the first sub-critical region of intake instability occurs at a mean mass flow ratio of about 0.85, irrespective of how the four individual throttles are set to achieve this ratio.

It is interesting to note the similarity between photographs (b), (e) and (h) of Fig.27, which show oscillation of the shock system at a mean mass flow ratio of about 0.85 and also between (a) and (d) which show stable flow at mean mass flow ratios of 0.87 and 0.88. These similarities in shock configuration at constant mean mass flow, indicate that the furthest forward position of part of the normal shock ahead of the inlet may be a function of the mean mass flow rather than the distribution of this mass flow.

4 FURTHER WORK

The design of intake used in the present investigation was relatively uncritical and it is possible that with a more highly developed intake the interference effects would be more far-reaching. It is intended therefore to follow this work with a further programme using a double-wedge, variable-geometry design with alternatively all-external compression and mixed external-internal compression.

5 CONCLUSIONS

From tests made at M = 2.0 on a single-wedge rectangular air intake feeding four side-by-side simulated engines, the following conclusions have been drawn:-

(1) When the throttles of all four cells are set to give critical inlet flow the mean pressure recovery in each cell is approximately 0.85.

(2) When the throttles of three cells are set at the critical inlet flow condition and the fourth is set to pass a reduced flow:-

(a) pressure recovery and mass flow ratio in each cell are reduced, the magnitudes of the reductions being progressively smaller in cells situated further from the throttled cell;

(b) the normal shock in front of the throttled cell is not as far ahead of the inlet as might be expected from the mass flow passing through that cell;

(c) the total quantity of air spilled from the intake is independent of which cell is throttled and is approximately 1.5 times the quantity of air spilled from the throttled cell.

(3) If one cell is throttled to pass reduced mass flow the mean pressure recovery in an adjacent cell is generally lower than that in the throttled cell.

(4) Division of the ducting upstream of a pair of cells has an influence on the performance of a cell adjacent to one which is throttled. Types of division tested were:-

A - duct divided from inlet plane;

B - duct divided from beginning of subsonic diffuser;

C - duct not divided.

It was found that:-

(a) lowest pressure recoveries in an adjacent cell were obtained with a type-B division;

(b) the average spillage from an adjacent cell for 0.57 spillage from the throttled cell was as follows:-

type-A division	0.095
type-B division	0.187
duct not divided (C)	0.125

(5) If the throttle of one cell is opened to give super-critical inlet flow, an adjacent cell is not affected if the ducting upstream of the cells is divided from the beginning of the subsonic diffuser. If the cells have a common diffuser, the adjacent cell suffers reductions in both pressure recovery and mass flow but the flow through the cell whose throttle is opened increases to values greater than the corresponding full intake flow.

(6) The first sub-critical region of intake instability occurs at a mean mass flow ratio of approximately 0.85, irrespective of how the four throttles are individually set to achieve this ratio.

(7) Further tests of a similar nature, but on a more highly-developed design of the basic intake, are intended.

REFERENCE

No.	Author	Title, etc
1	Campbell, R.C.	Performance of supersonic ramp-type side inlet with combinations of fuselage and inlet throat boundary-layer removal. NACA RME 56A17 TIL 5200. April 1956.

Printed in England for Her Majesty's Stationery Office by the Royal Aircraft Establishment, Farnborough. W.T 60.K.4

$\frac{w_{en}}{h_{en}} = 8$ (w_{en} = INTAKE WIDTH)

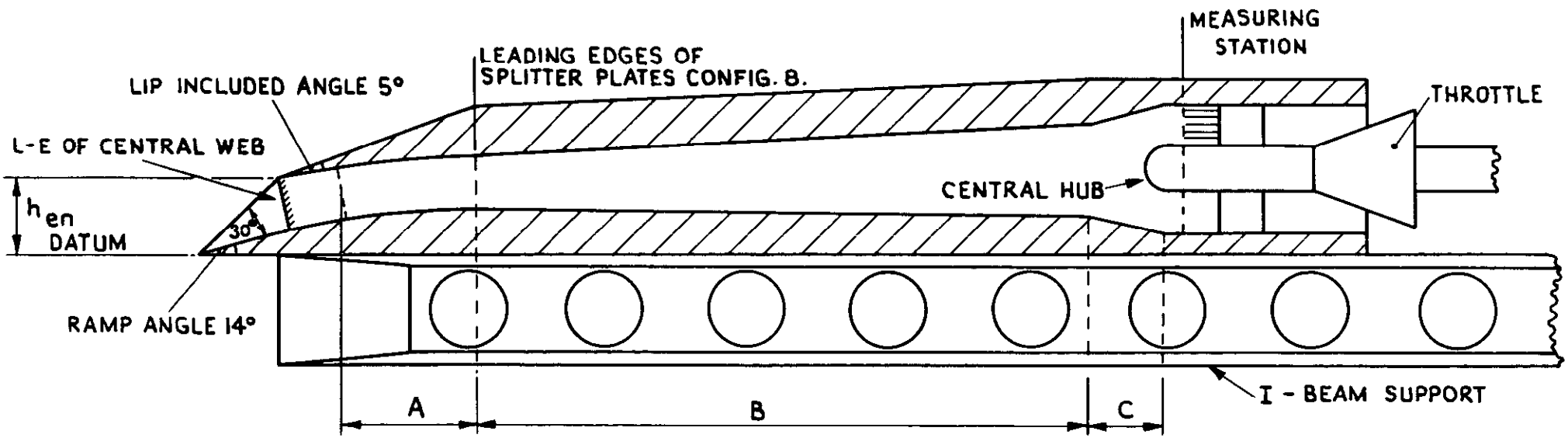

FIG.I. OUTLINE DRAWING OF MODEL.

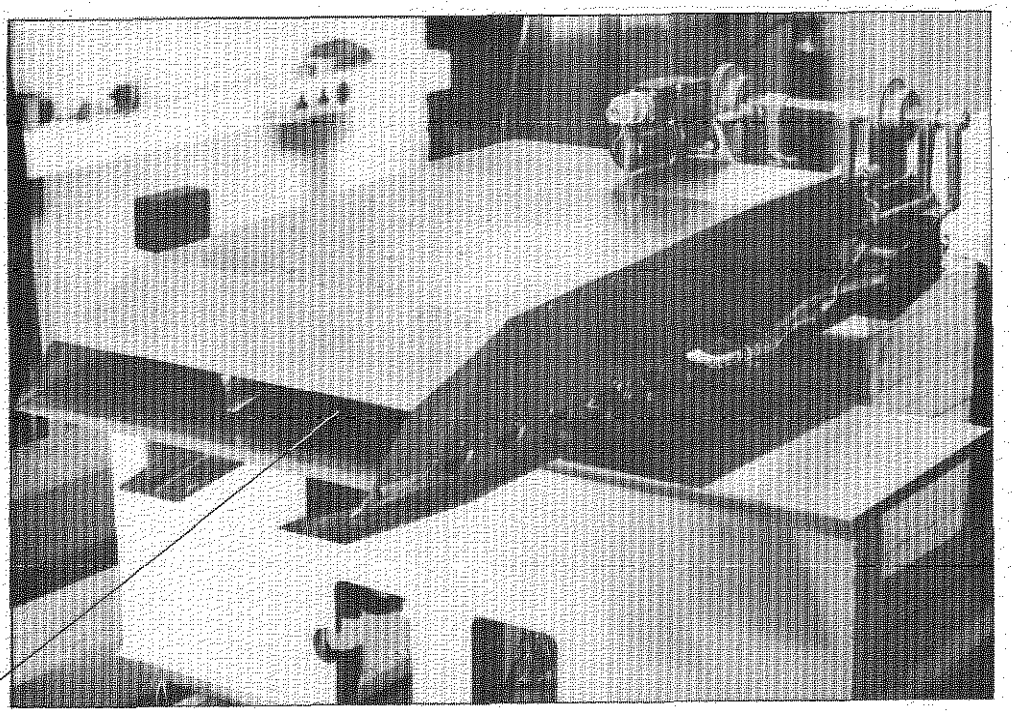

RECTANGULAR FIXED GEOMETRY INLET FEEDING FOUR SIDE BY SIDE ENGINES

a. GENERAL VIEW

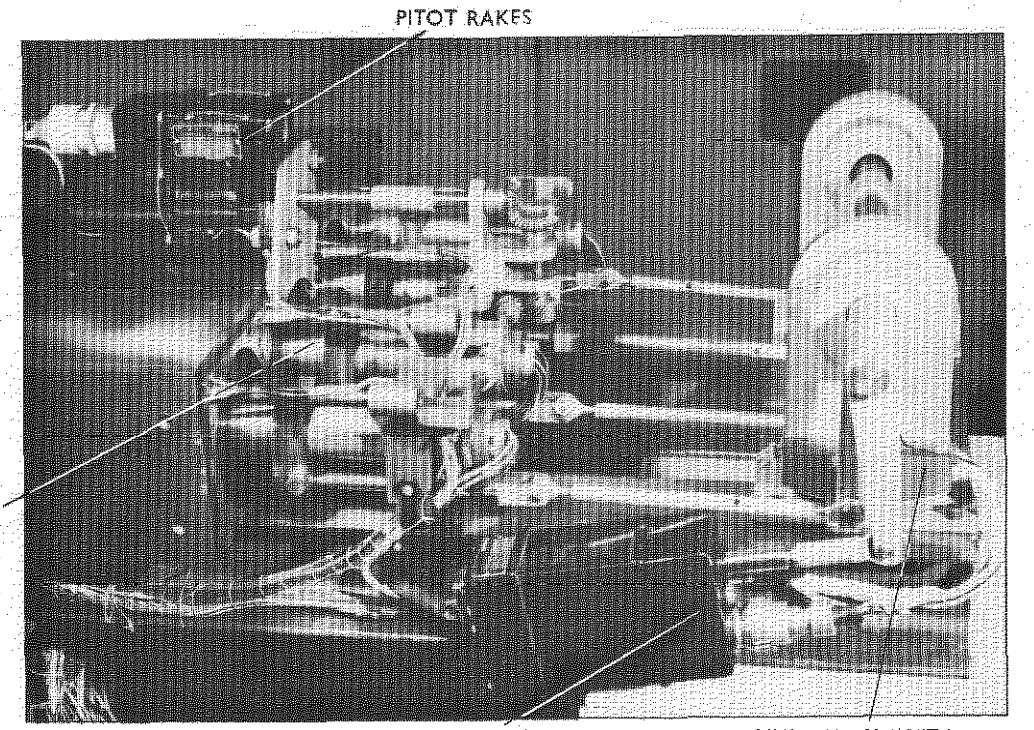

ROTARY ACTUATOR FOR ROTATING PITOT RAKES

MASS FLOW THROTTLES

LINEAR ACTUATOR FOR ADJUSTING MASS FLOW THROTTLES

MULTI-WAY SWITCH FOR INDICATING POSITION OF MASS FLOW THROTTLES

b. VIEW OF REAR SHOWING THE VARIOUS MECHANISMS

FIG.2. MODEL

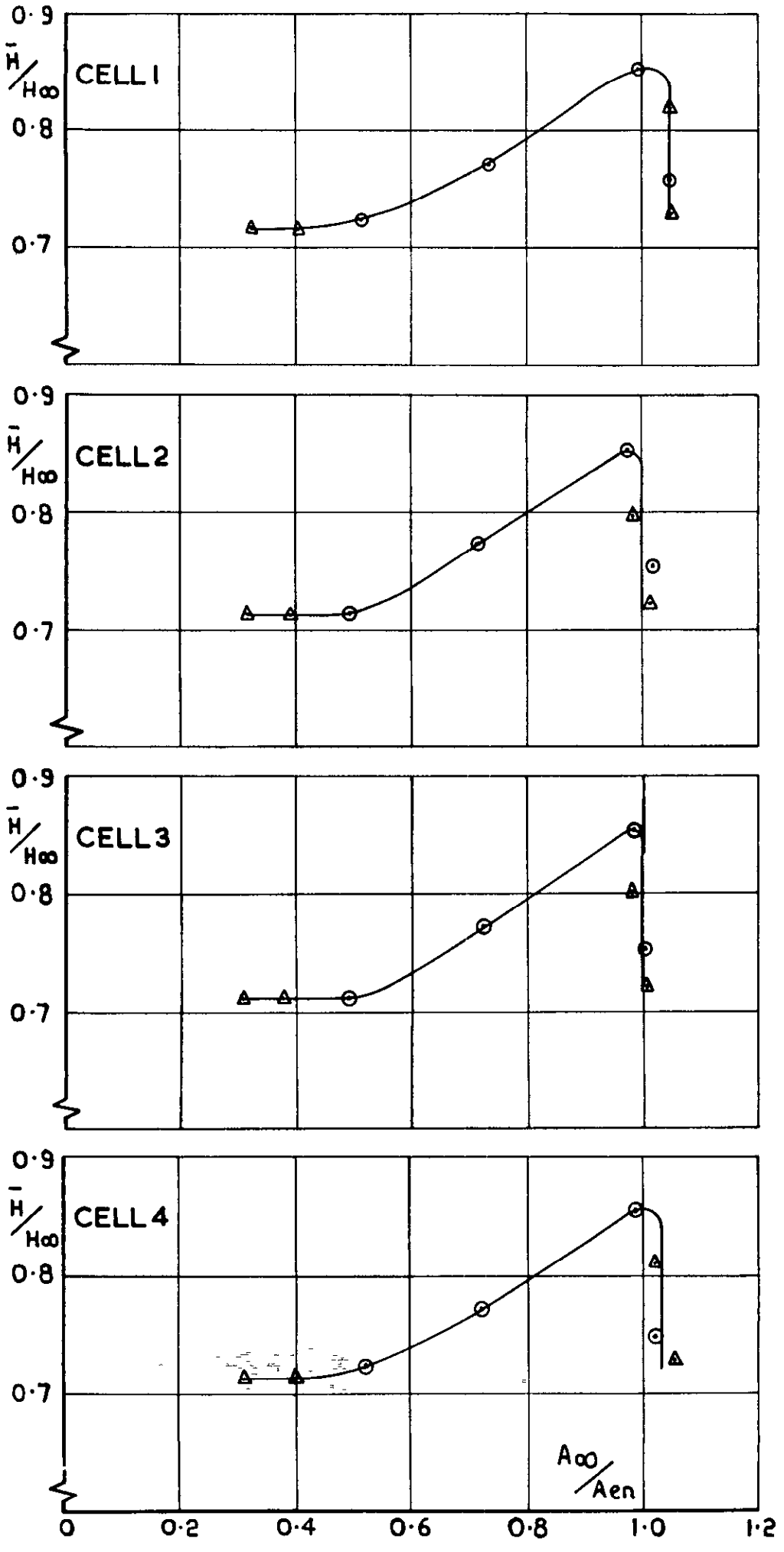

FIG. 3. VARIATION OF PRESSURE RECOVERY WITH MASS FLOW RATIO, CONFIGURATION A, FOUR CELLS THROTTLED TOGETHER.

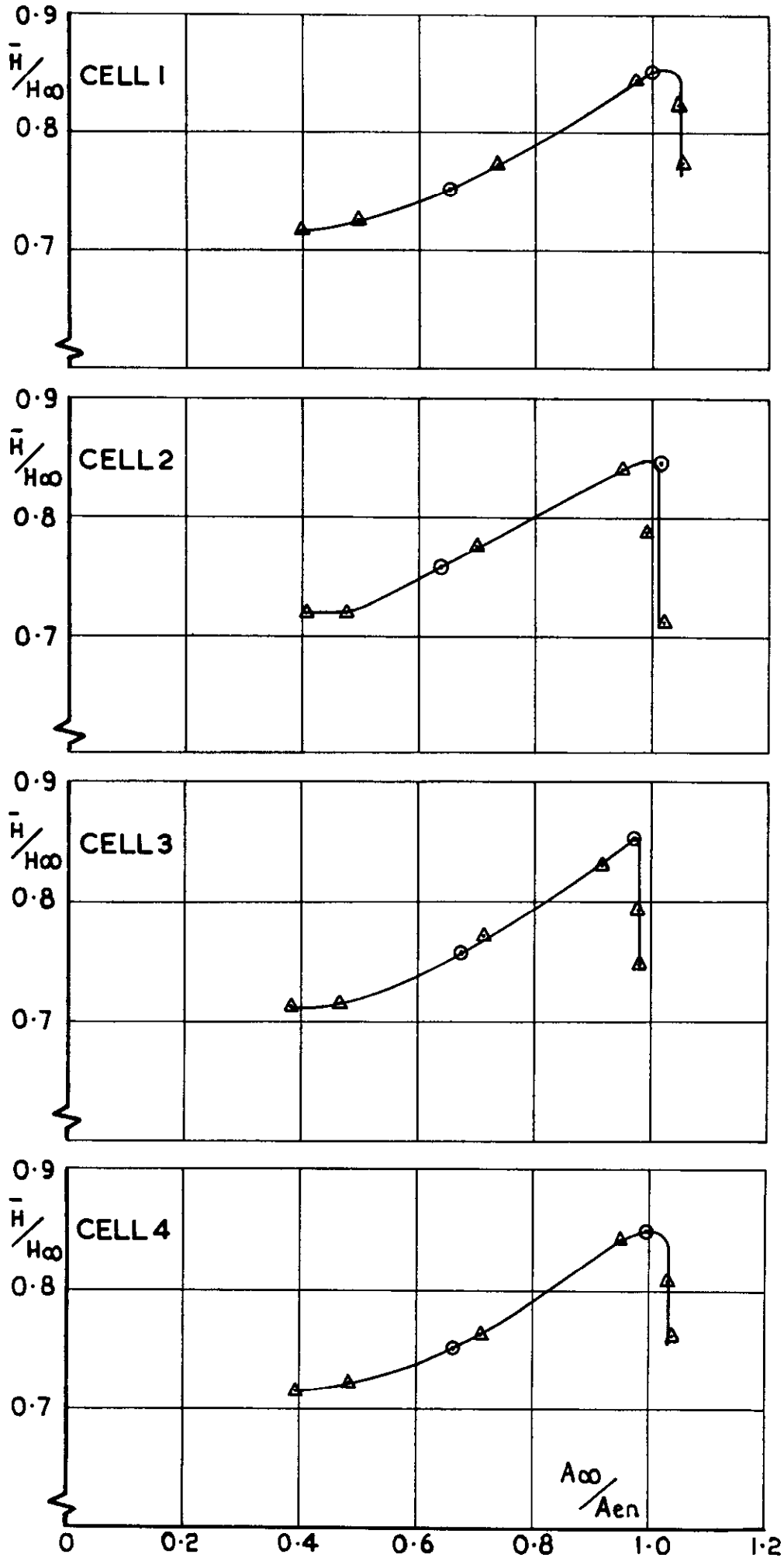

FIG. 4. VARIATION OF PRESSURE RECOVERY WITH MASS FLOW RATIO, CONFIGURATION B, FOUR CELLS THROTTLED TOGETHER.

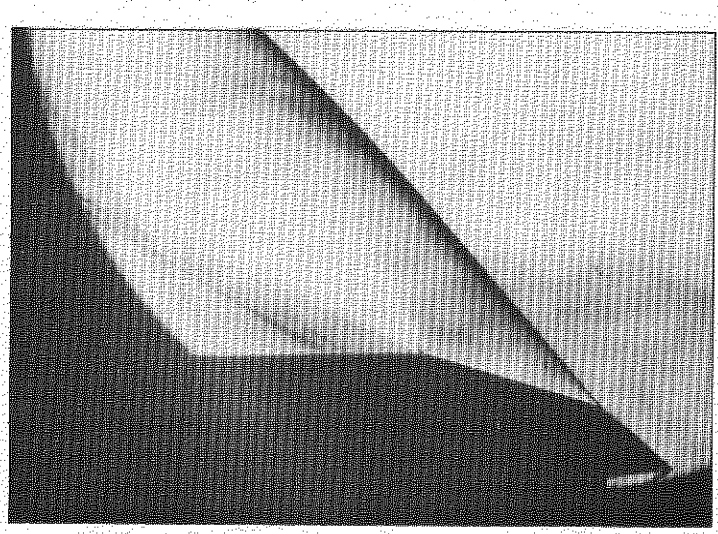

(a) $A_\infty / A_{en} \triangleq 1.0$

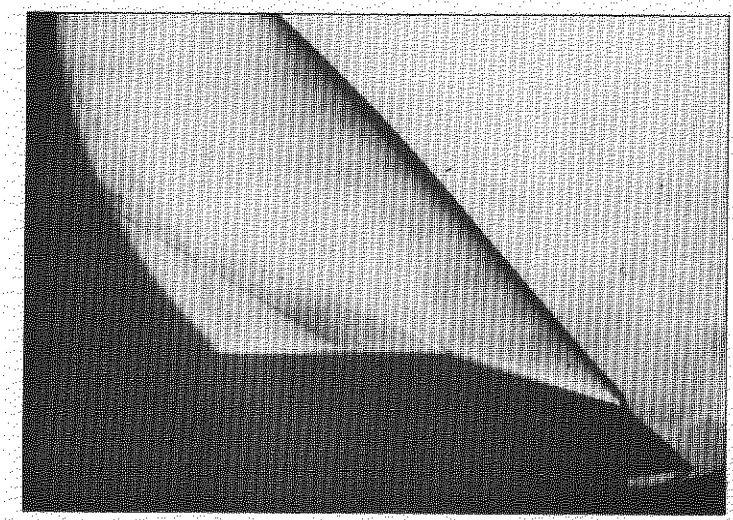

(b) $A_\infty / A_{en} \triangleq 0.98$

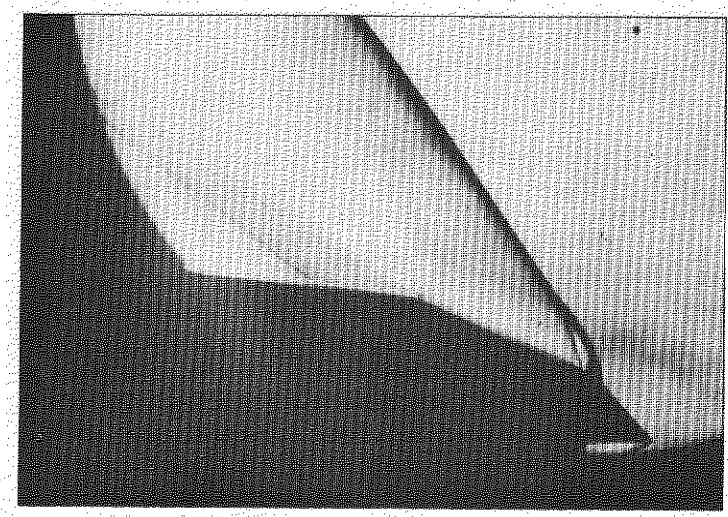

(c) $A_\infty / A_{en} \triangleq 0.91$

FIG.5. SCHLIEREN PHOTOGRAPHS. CONFIGURATION A, WITH ALL FOUR CELLS THROTTLED TOGETHER

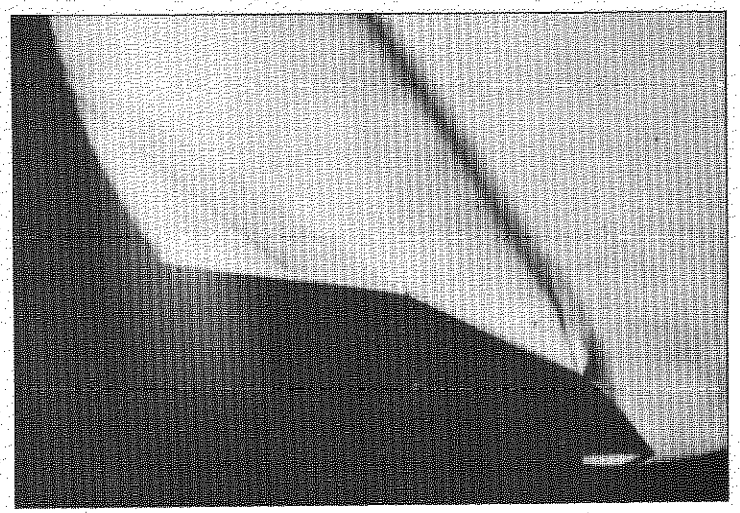

(d) $A_\infty / A_{en} \simeq 0.85$

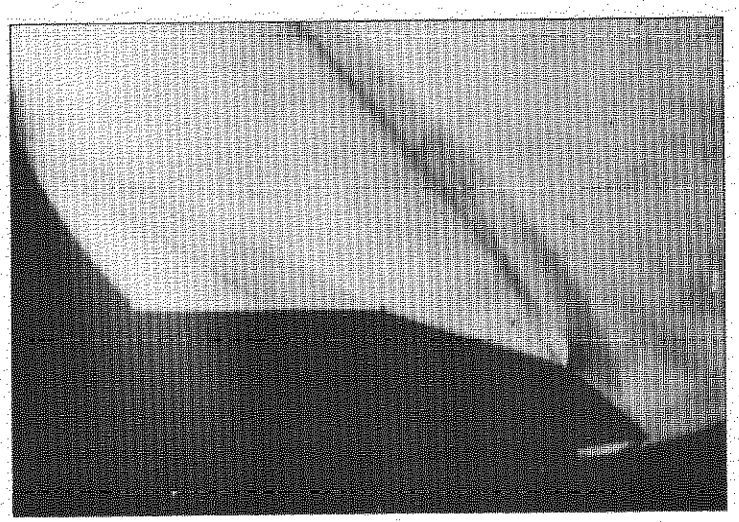

(e) $A_\infty / A_{en} \simeq 0.78$

FIG.5 (continued)

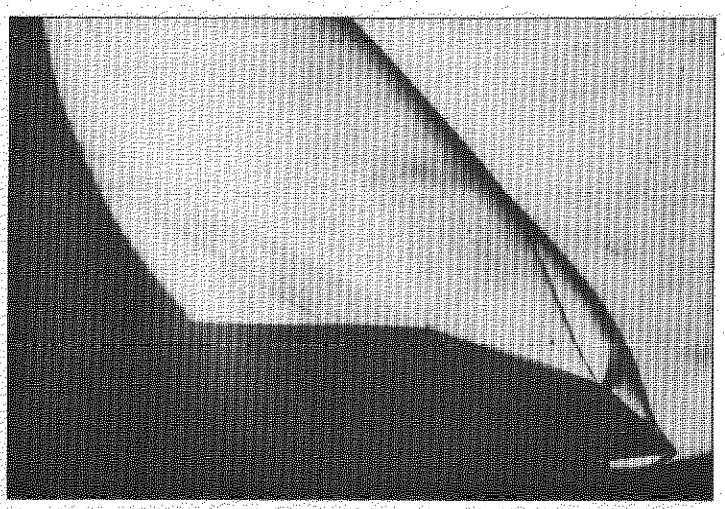

(f) $A_\infty/A_{en} \triangleq 0.72$

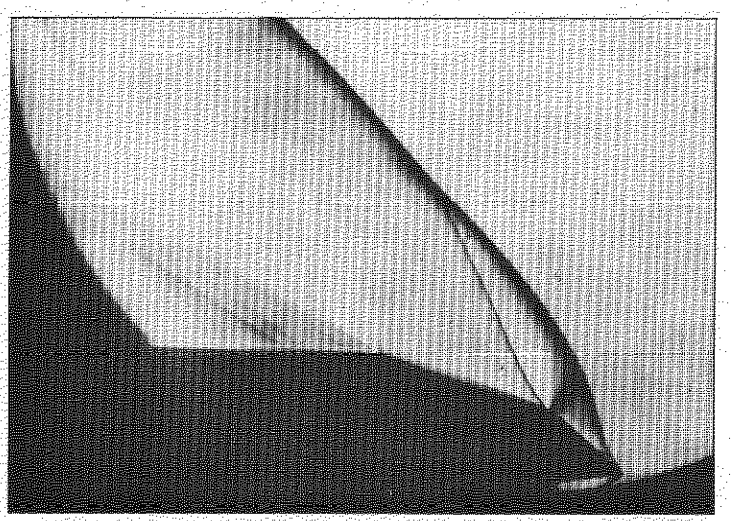

(g) $A_\infty/A_{en} \triangleq 0.67$

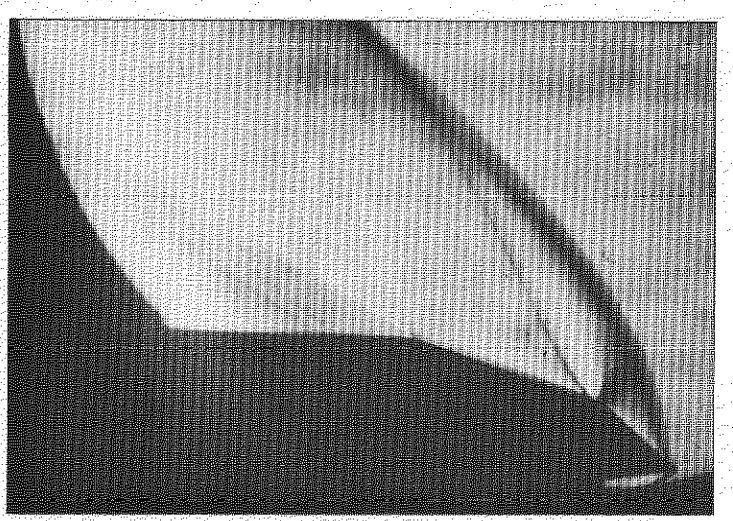

(h) $A_\infty/A_{en} \triangleq 0.62$

FIG.5 (continued)

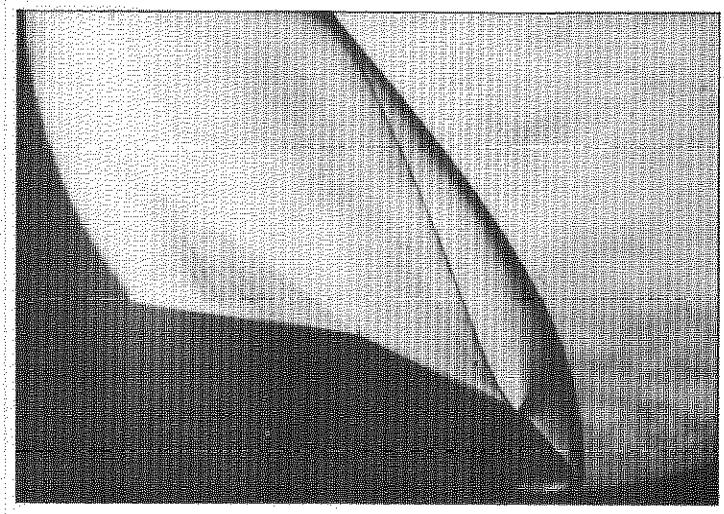

(i) $A_\infty/A_{en} \triangleq 0.56$

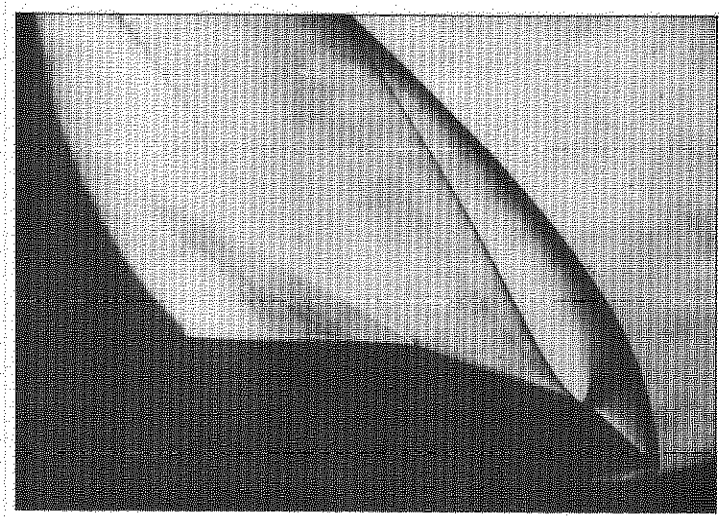

(j) $A_\infty/A_{en} \triangleq 0.50$

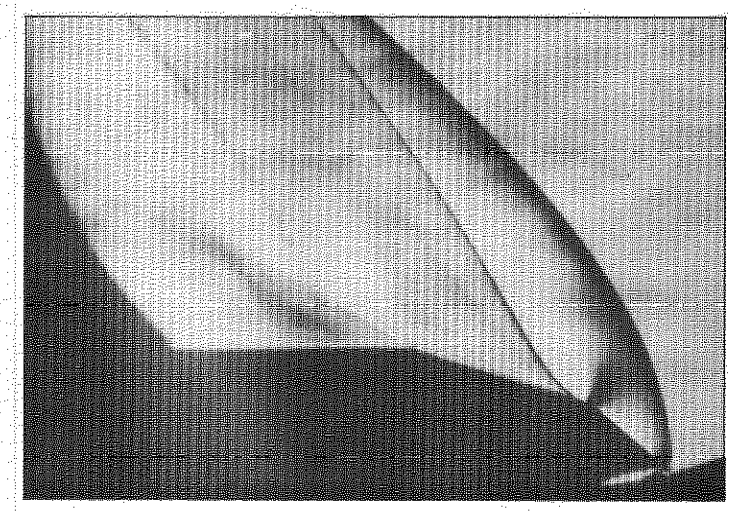

(k) $A_\infty/A_{en} \triangleq 0.39$

FIG.5. (concluded)

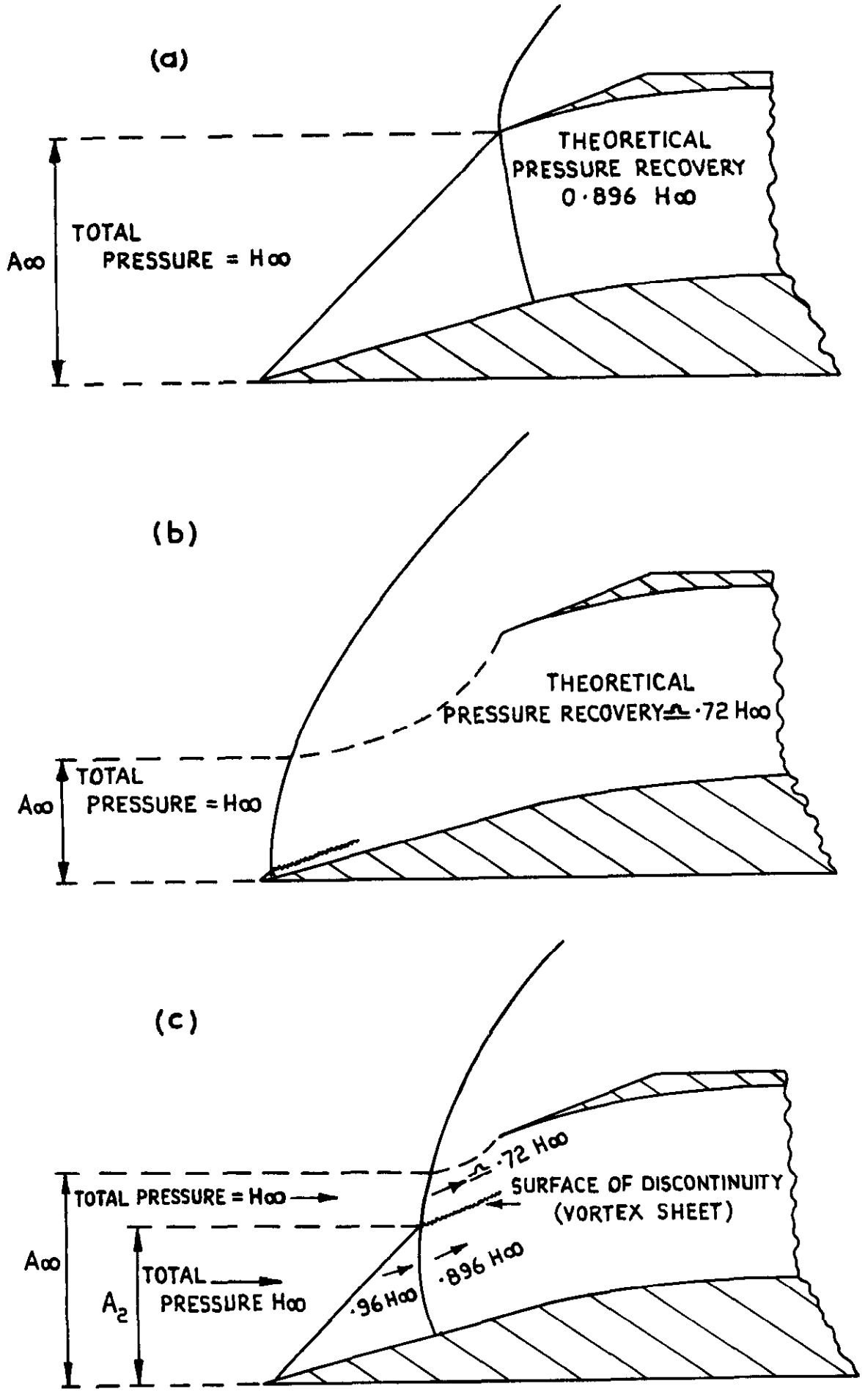

FIG. 6. SKETCHES OF SHOCK CONFIGURATIONS SHOWING HOW VARIATION OF $\bar{H}/H_\infty$ WITH A_∞/A_{en} IS ACHIEVED.

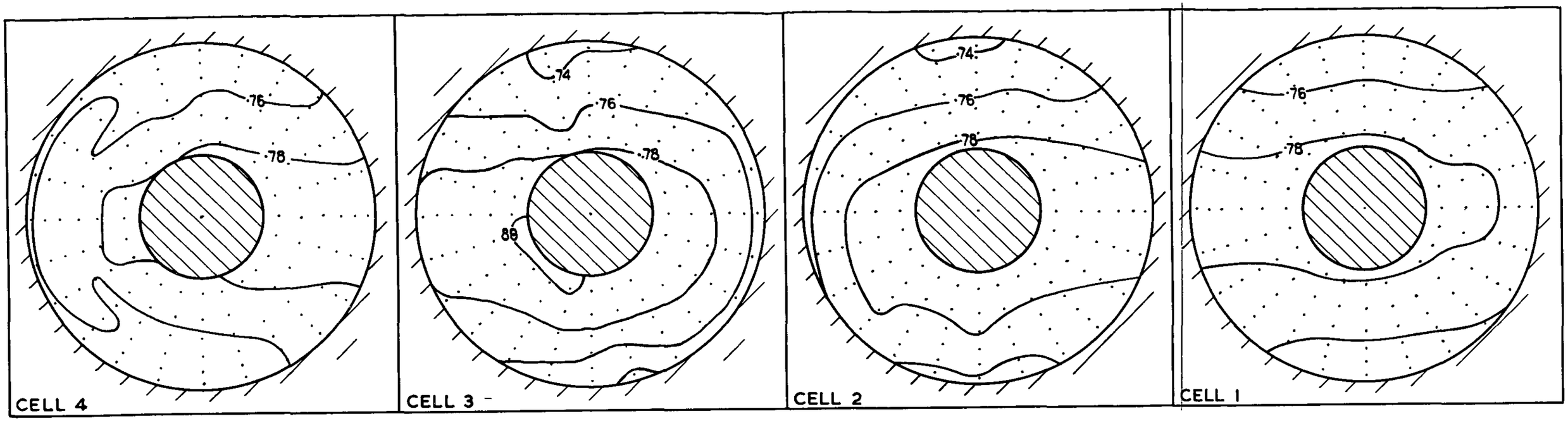

(a) $A_\infty/A_{en} \simeq 0.72$, $\bar{H}/H_\infty \simeq 0.77$.

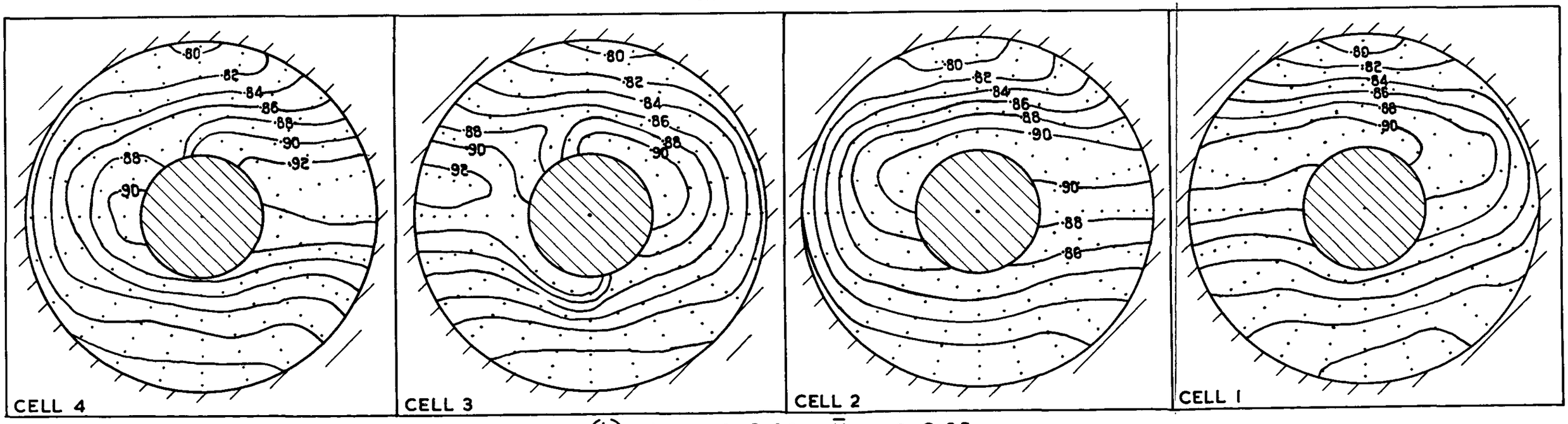

(b) $A_\infty/A_{en} \simeq 0.99$, $\bar{H}/H_\infty \simeq 0.85$.

FIG. 7. TOTAL PRESSURE DISTRIBUTIONS LOOKING DOWNSTREAM, CONFIGURATION A
(A_∞/A_{en} & $\bar{H}/H_\infty$ ARE THE MEAN VALUES FOR THE FOUR CELLS.)

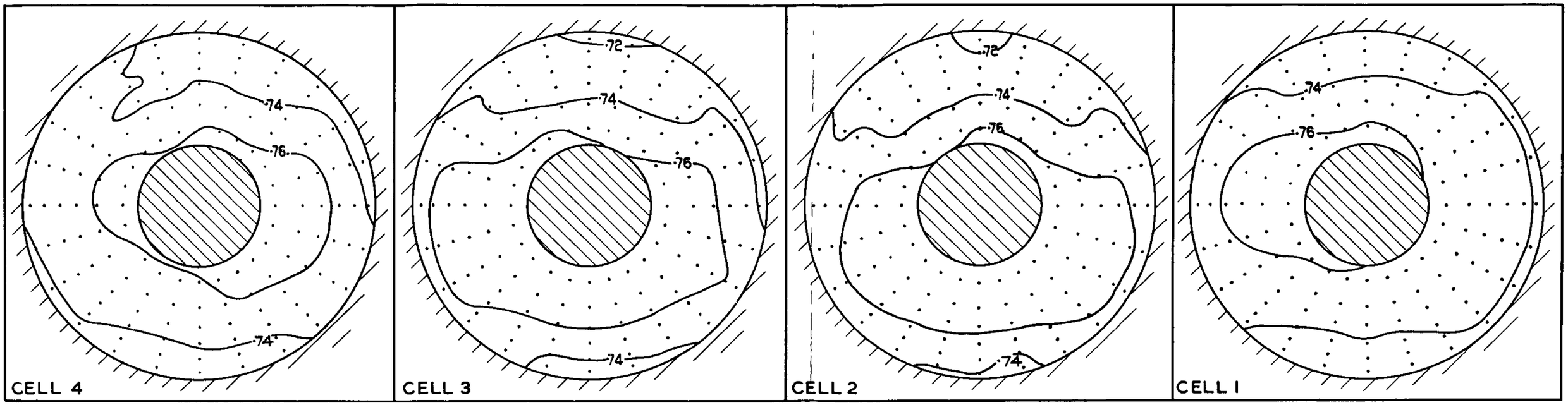

(a) $A_\infty/A_{en} \simeq 0.66$; $\bar{H}/H_\infty \simeq 0.75$.

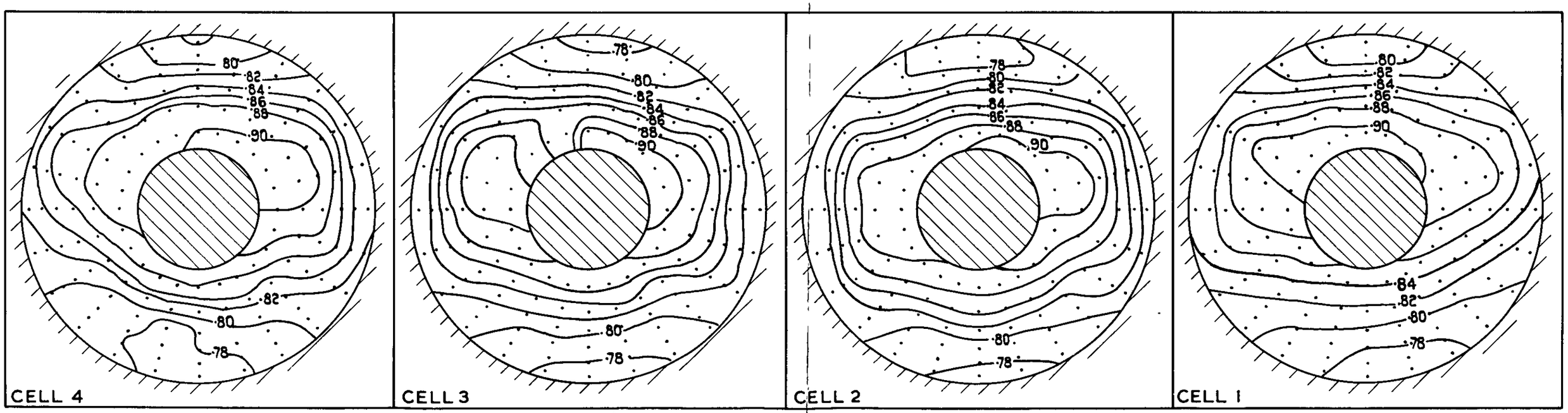

(b) $A_\infty/A_{en} \simeq 0.99$, $\bar{H}/H_\infty \simeq 0.85$.

FIG 8. TOTAL PRESSURE DISTRIBUTIONS LOOKING DOWNSTREAM, CONFIGURATION B.
(A_∞/A_{en} & $\bar{H}/H_\infty$ ARE THE MEAN VALUES FOR THE FOUR CELLS)

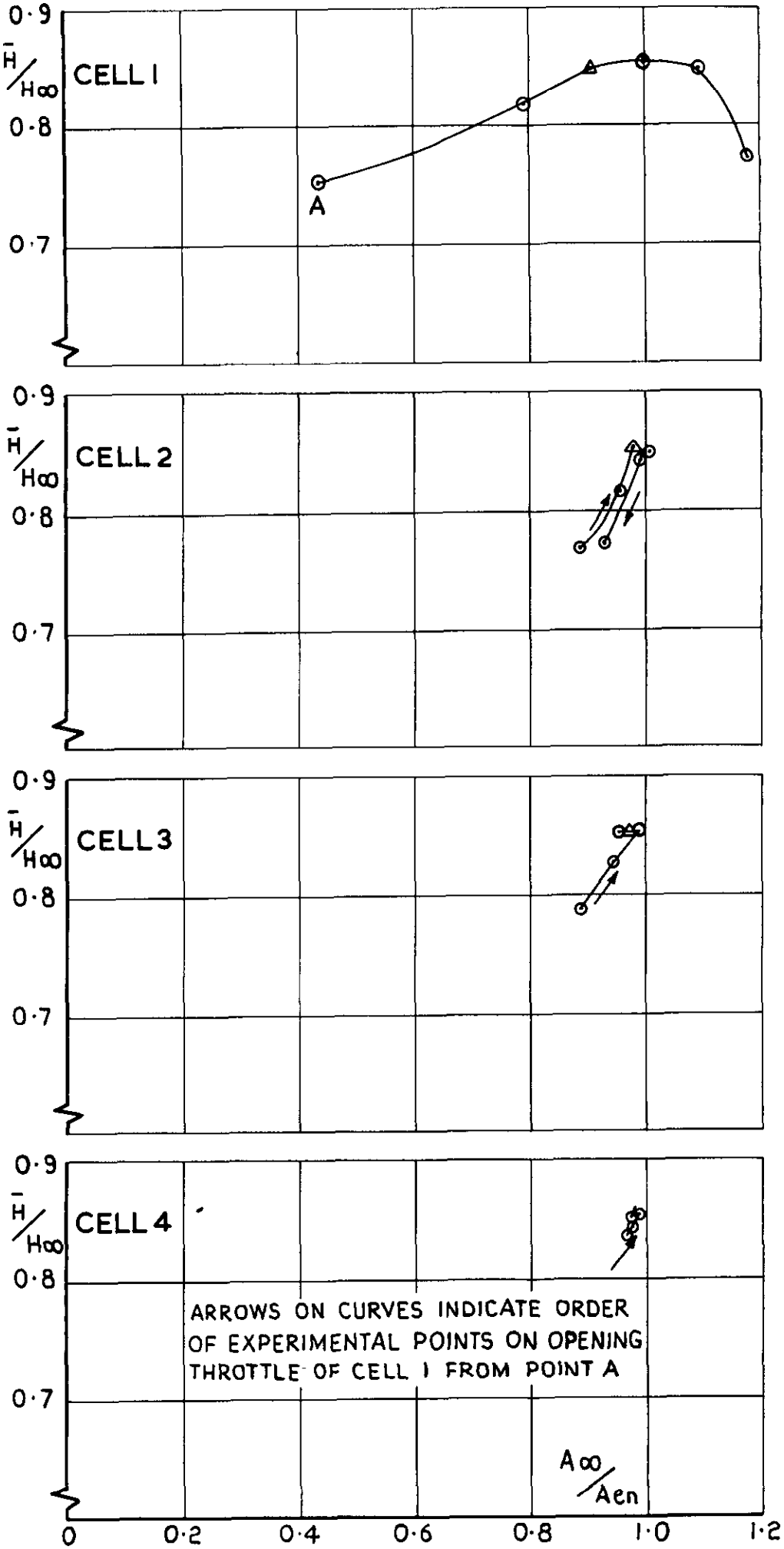

FIG. 9. VARIATION OF PRESSURE RECOVERY WITH MASS FLOW RATIO, CONFIGURATION A, CELL 1 THROTTLED.

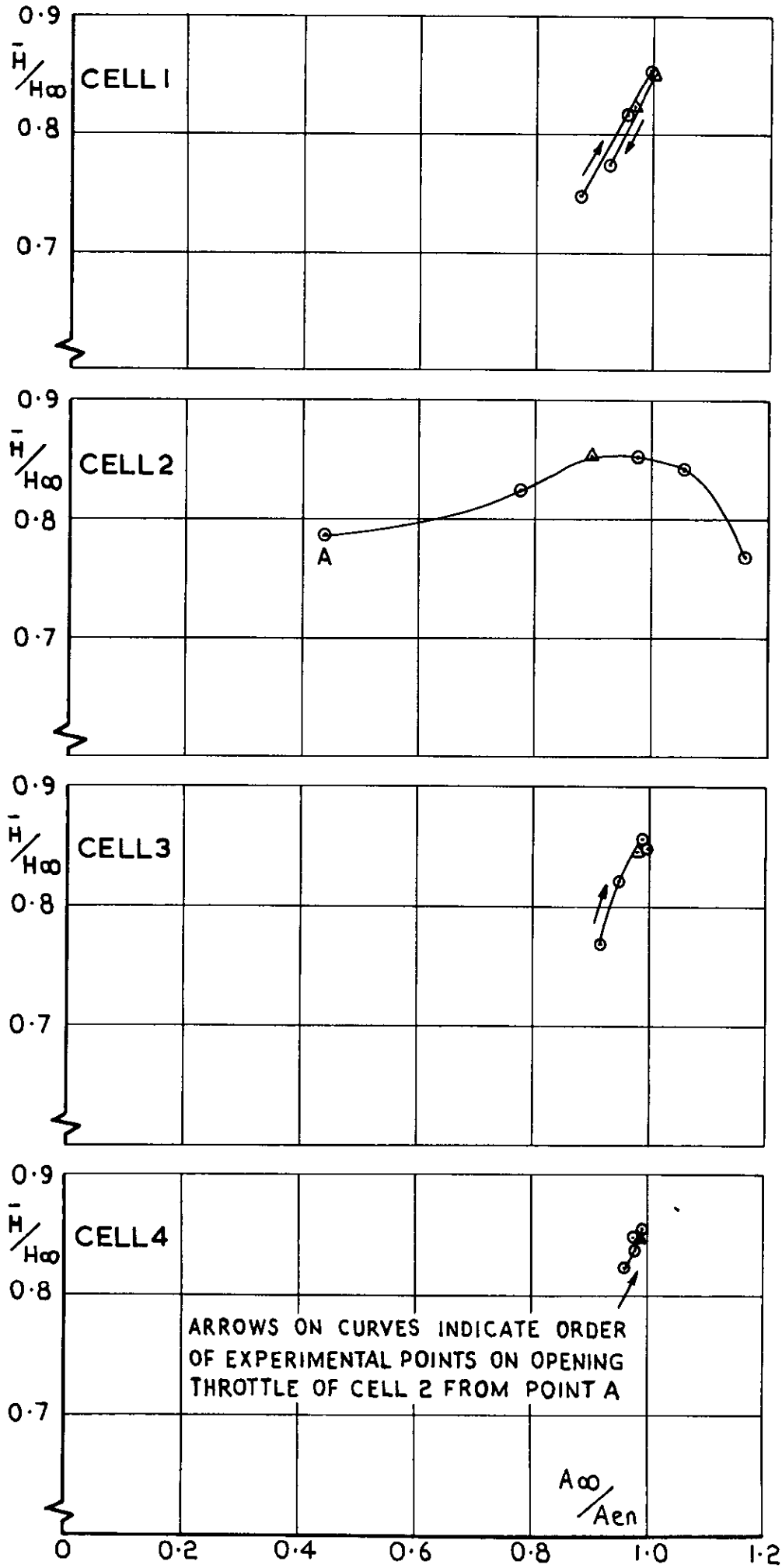

FIG.10. VARIATION OF PRESSURE RECOVERY WITH MASS FLOW RATIO, CONFIGURATION A, CELL 2 THROTTLED.

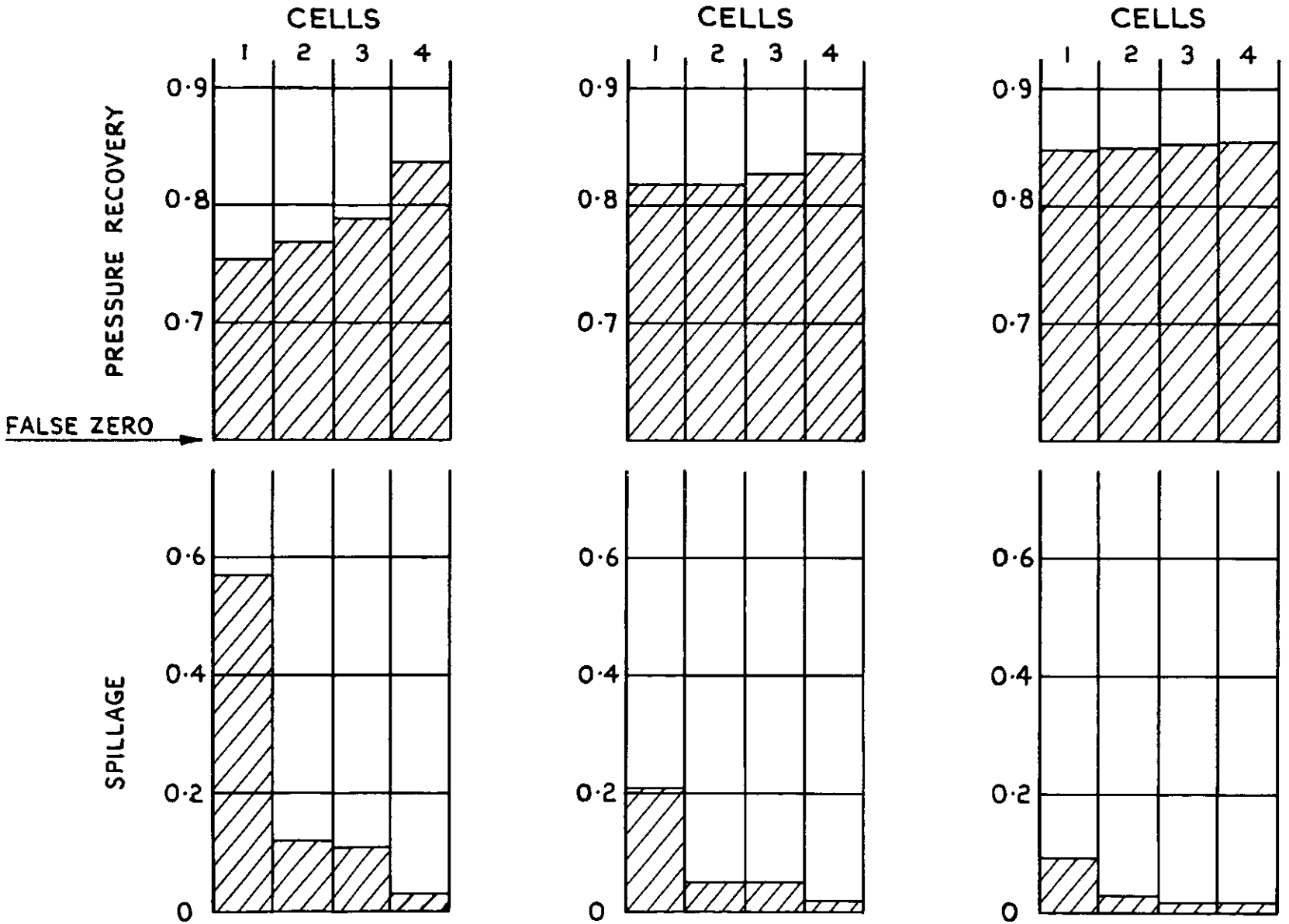

FIG. 11. BLOCK DIAGRAMS SHOWING PRESSURE RECOVERY & SPILLAGE IN CELLS WHEN CELL 1 IS THROTTLED, CONFIGURATION A.

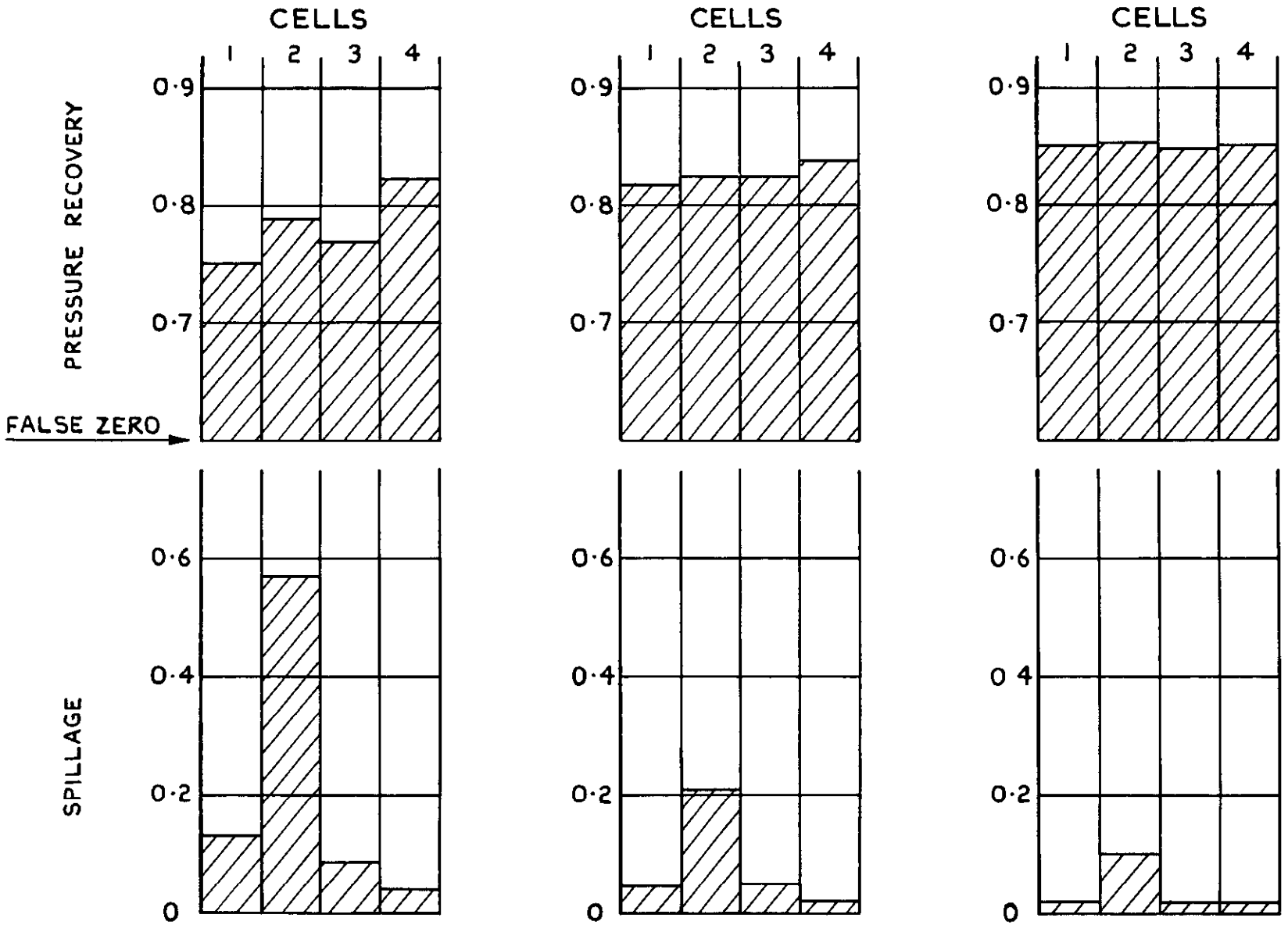

FIG. 12. BLOCK DIAGRAM SHOWING PRESSURE RECOVERY & SPILLAGE IN CELLS WHEN CELL 2 IS THROTTLED. CONFIGURATION A.

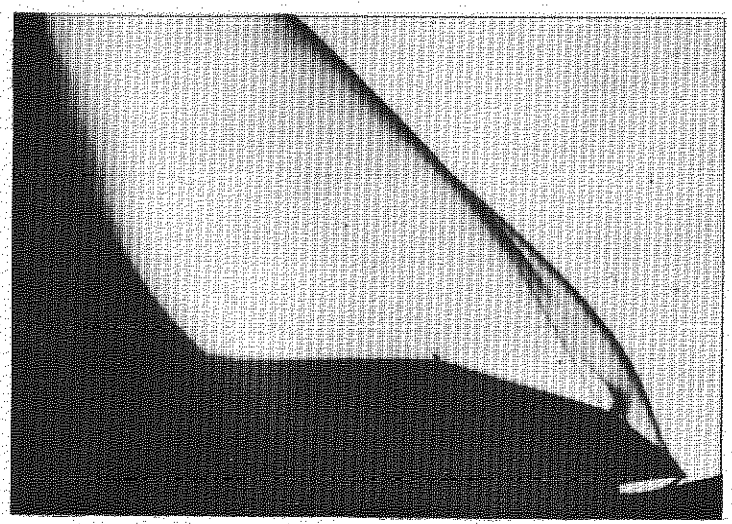

ONFIGURATION A, CELL 1 THROTTLED TO $A_\infty/A_{en} \doteq 0.43$

FIG.13. SCHLIEREN PHOTOGRAPH

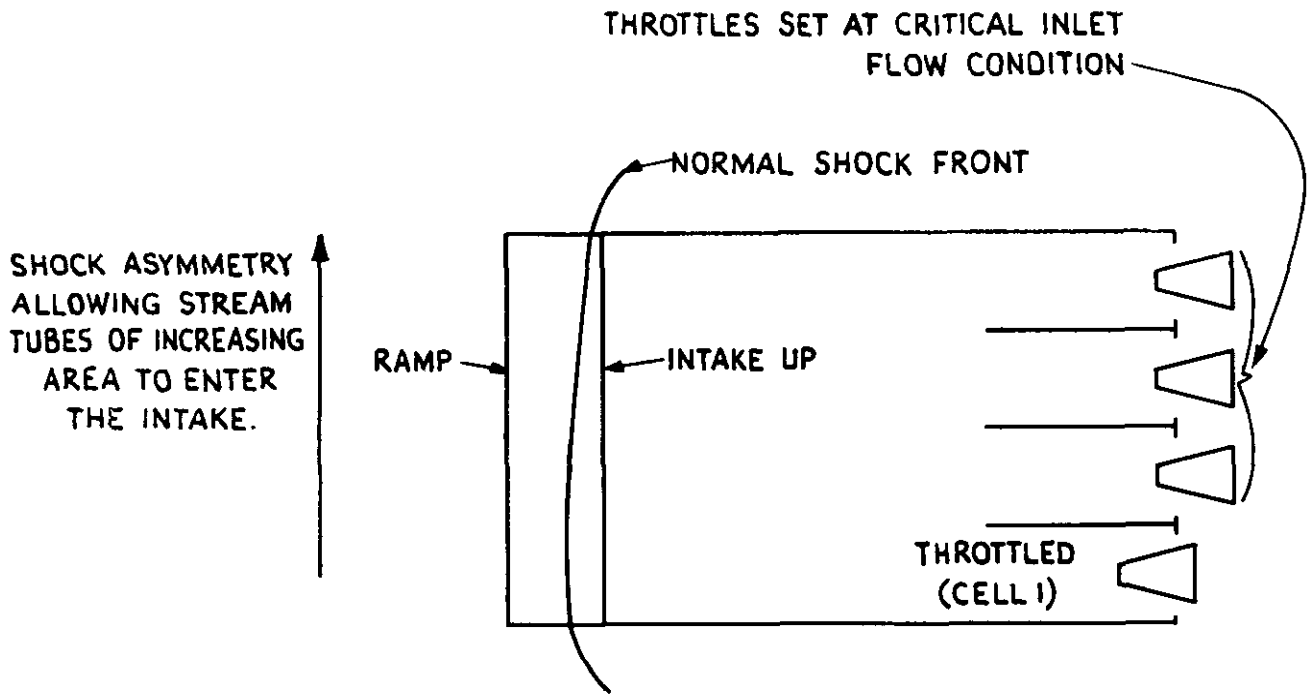

PLAN VIEW.

FIG. 14. SKETCH SHOWING ASYMMETRIC NORMAL SHOCK FRONT WHEN CELL 1 IS THROTTLED.

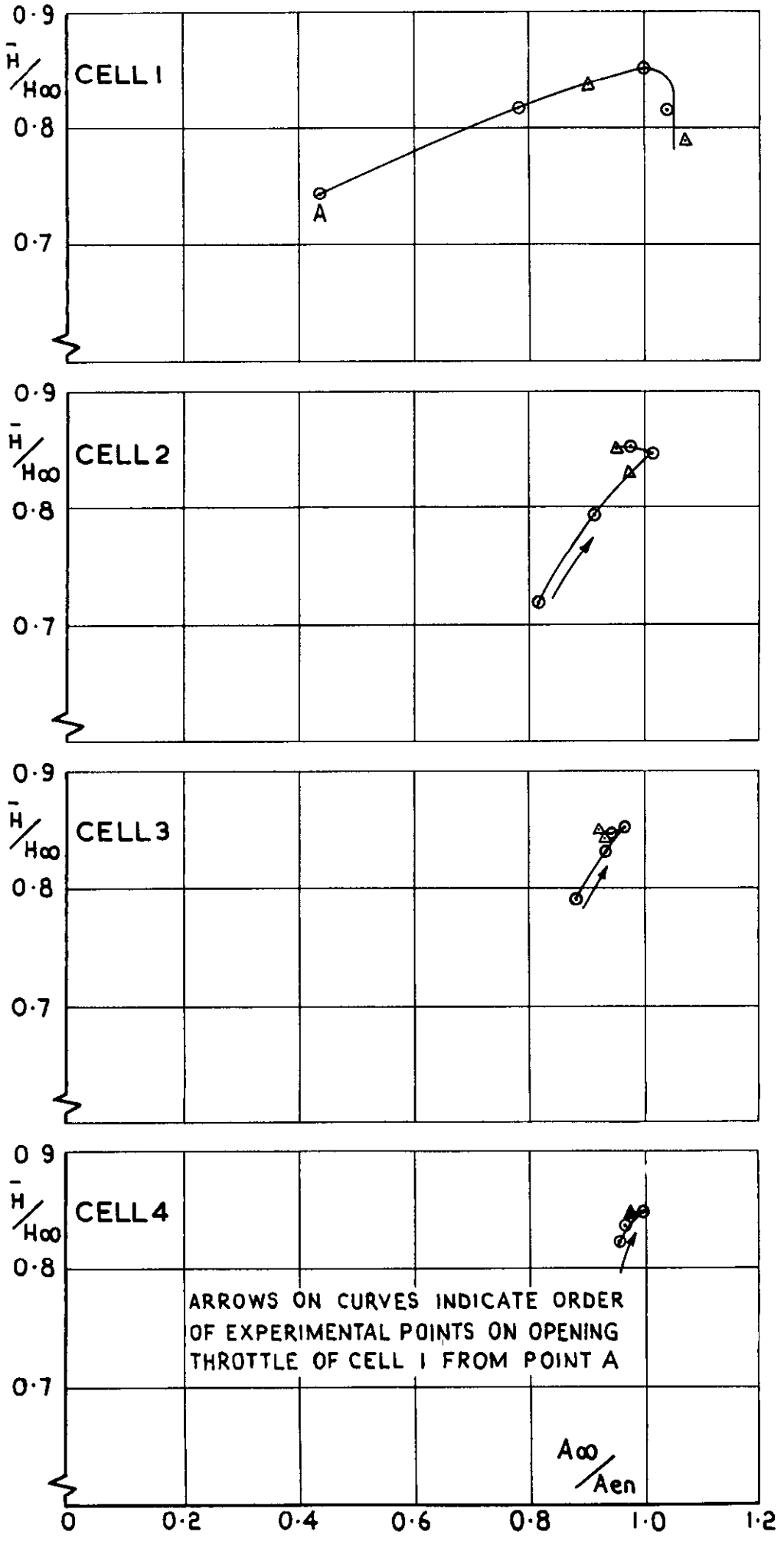

FIG.15. VARIATION OF PRESSURE RECOVERY WITH MASS FLOW RATIO, CONFIGURATION B, CELL 1 THROTTLED.

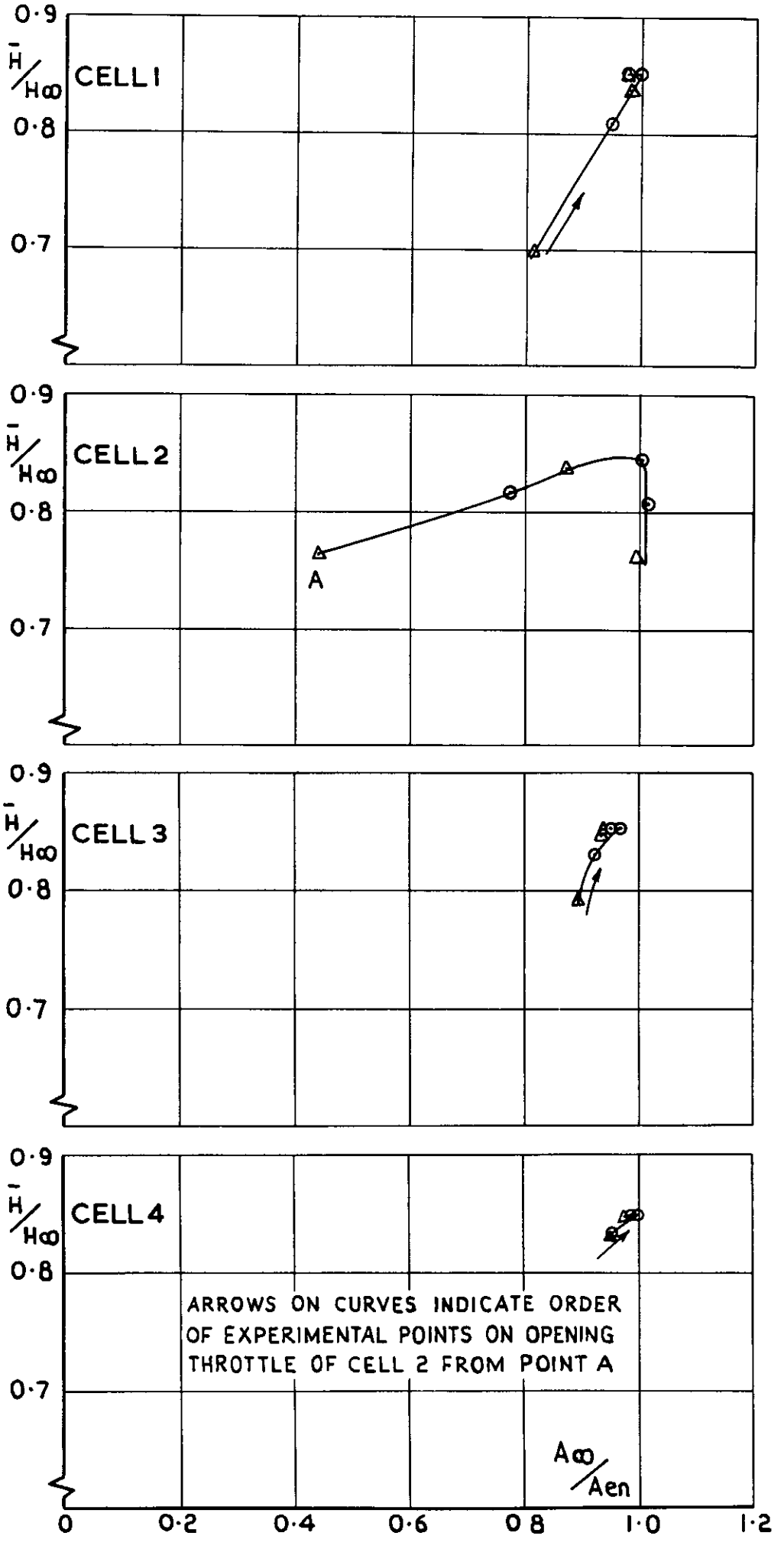

FIG.16. VARIATION OF PRESSURE RECOVERY WITH MASS FLOW RATIO, CONFIGURATION B, CELL 2 THROTTLED.

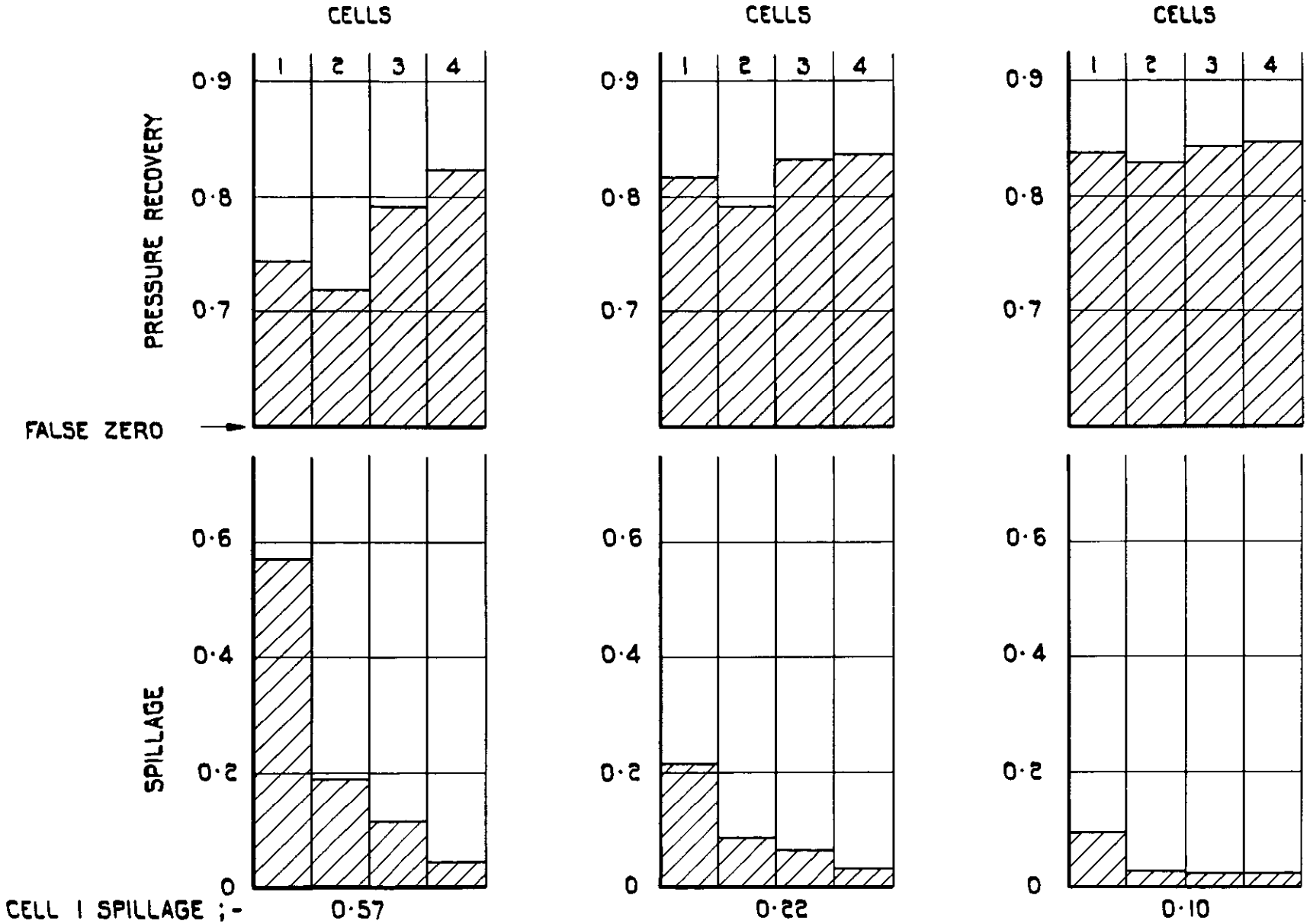

FIG 17. BLOCK DIAGRAMS SHOWING PRESSURE RECOVERY & SPILLAGE IN CELLS WHEN CELL 1 IS THROTTLED, CONFIGURATION B.

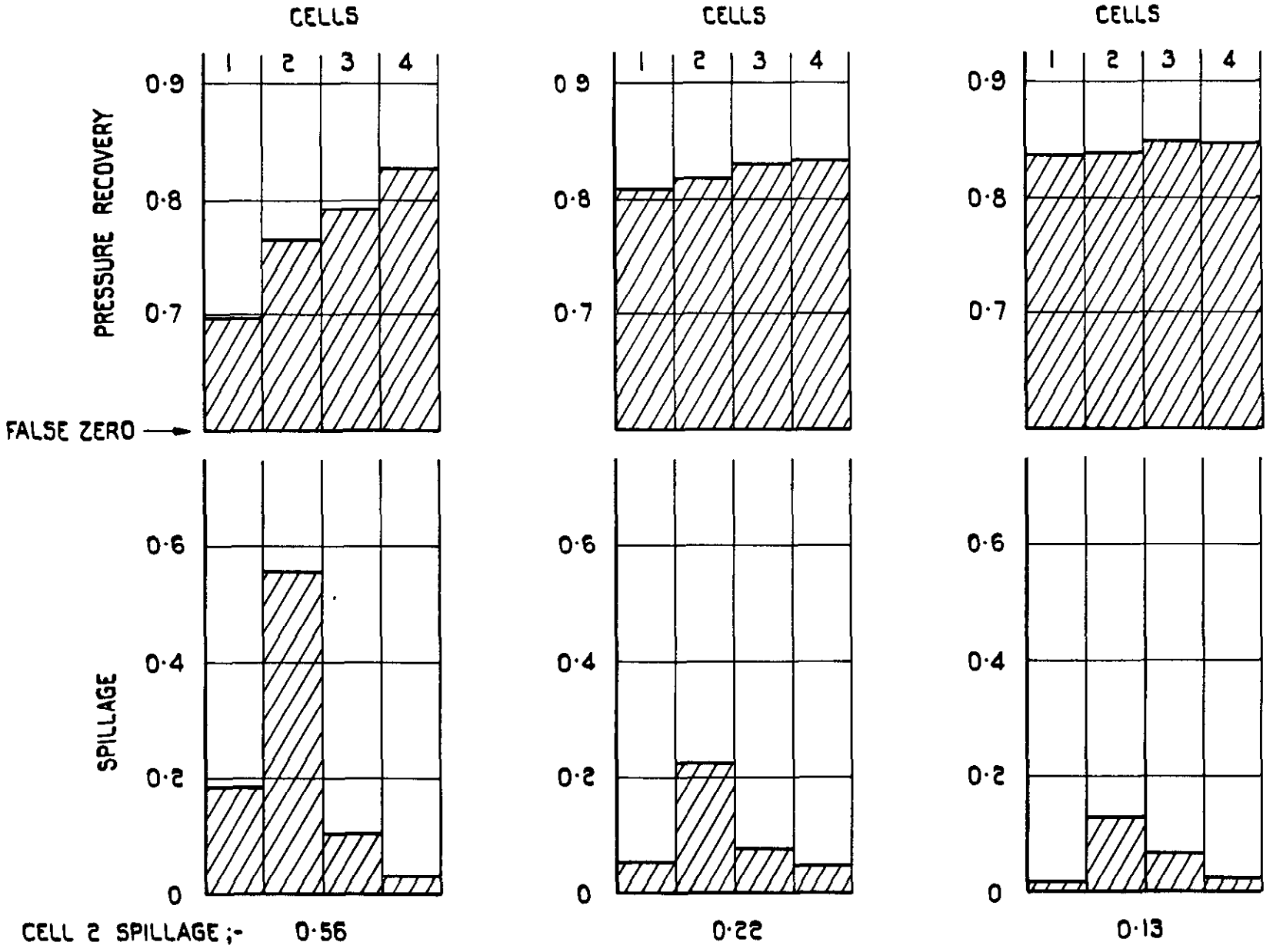

FIG. 18. BLOCK DIAGRAMS SHOWING PRESSURE RECOVERY & SPILLAGE IN CELLS WHEN CELL 2 IS THROTTLED. CONFIGURATION B.

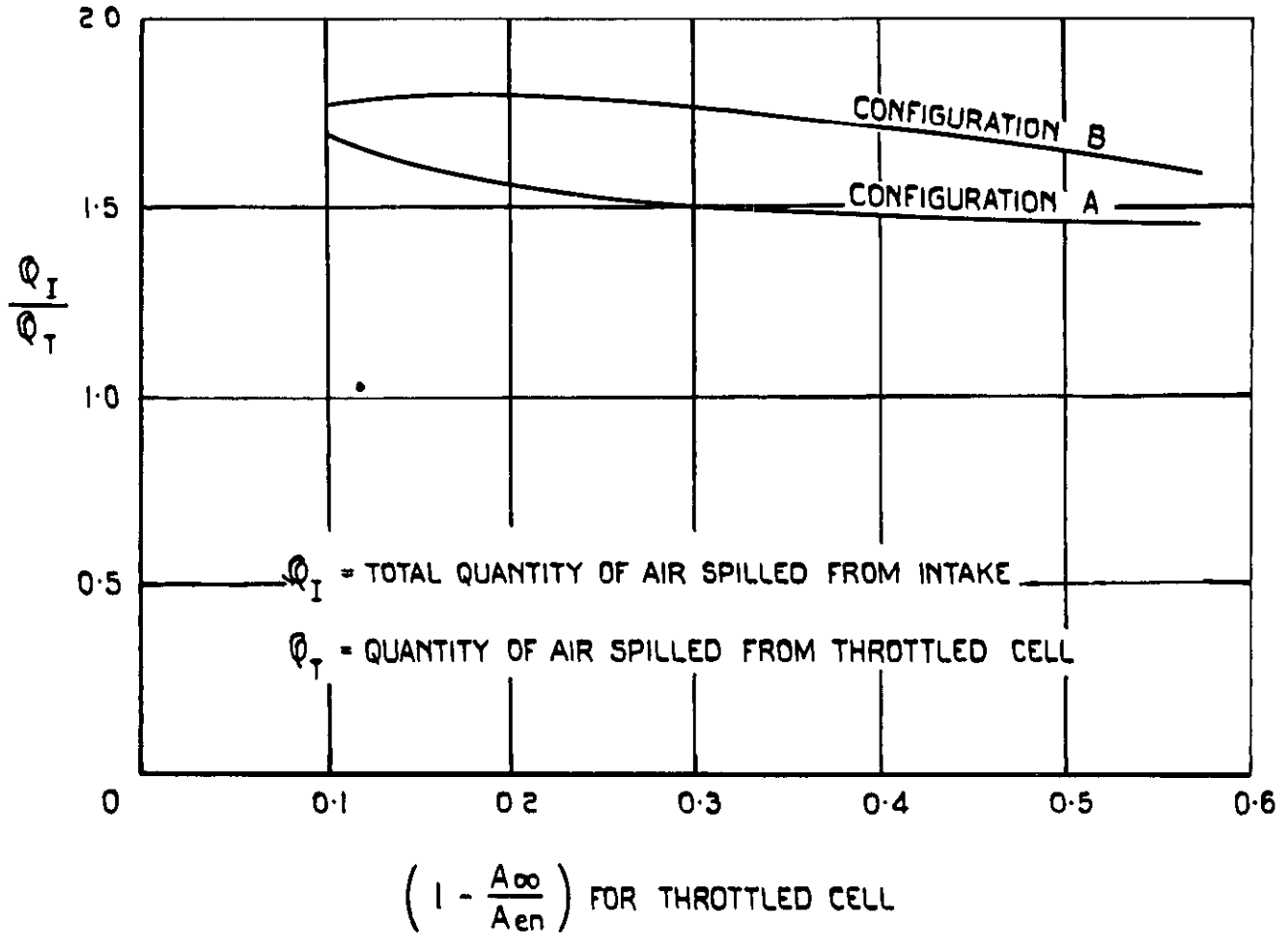

FIG. 19. $\frac{\varphi_I}{\varphi_T}$ – VARIATION WITH SPILLAGE FROM THROTTLED CELL.

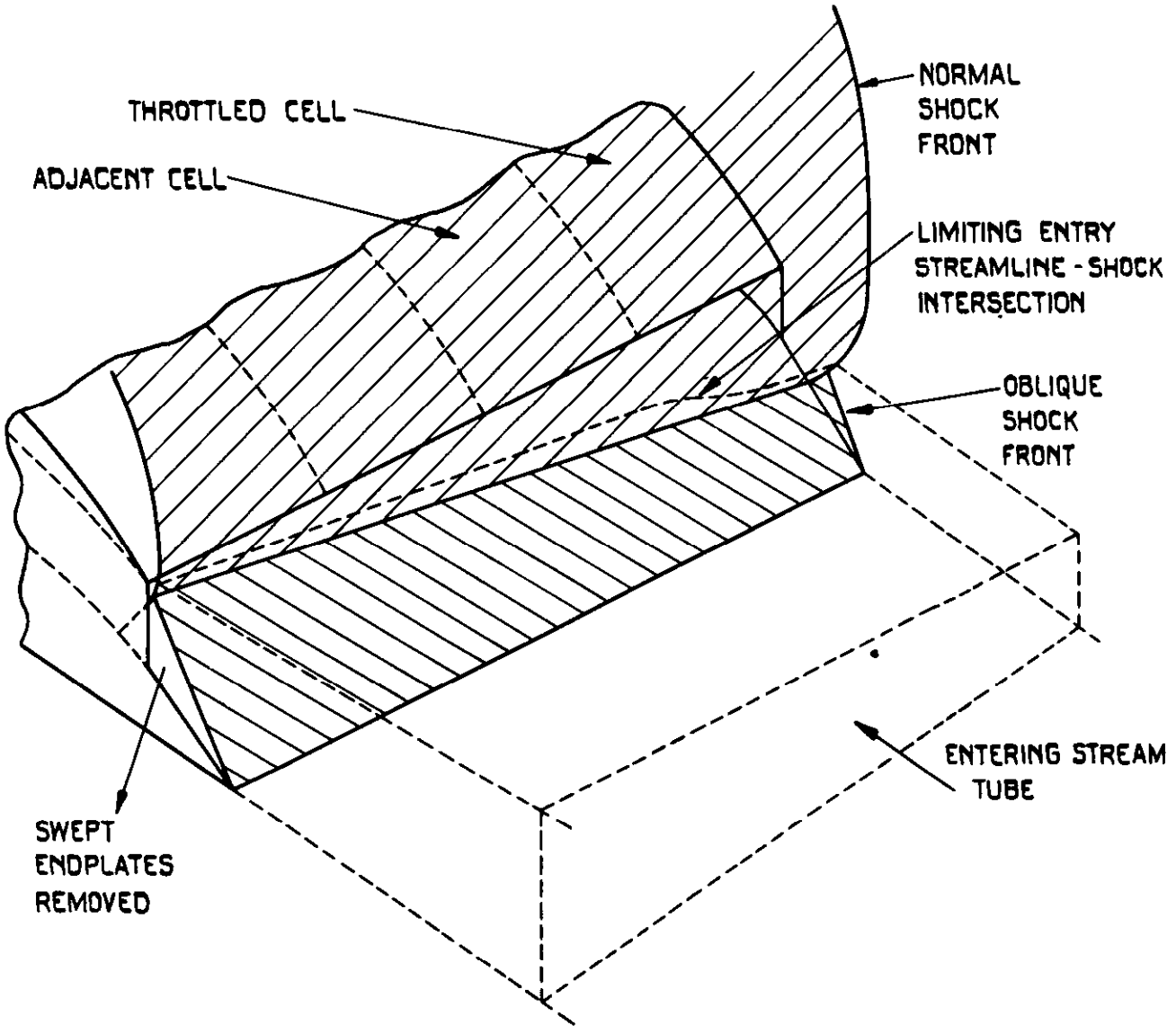

FIG. 20. VARIATION ACROSS THE INLET SPAN OF THE RELATIVE POSITION OF THE INTERSECTIONS OF THE OBLIQUE & NORMAL SHOCKS & THE LIMITING ENTRY STREAMLINE & NORMAL SHOCK.

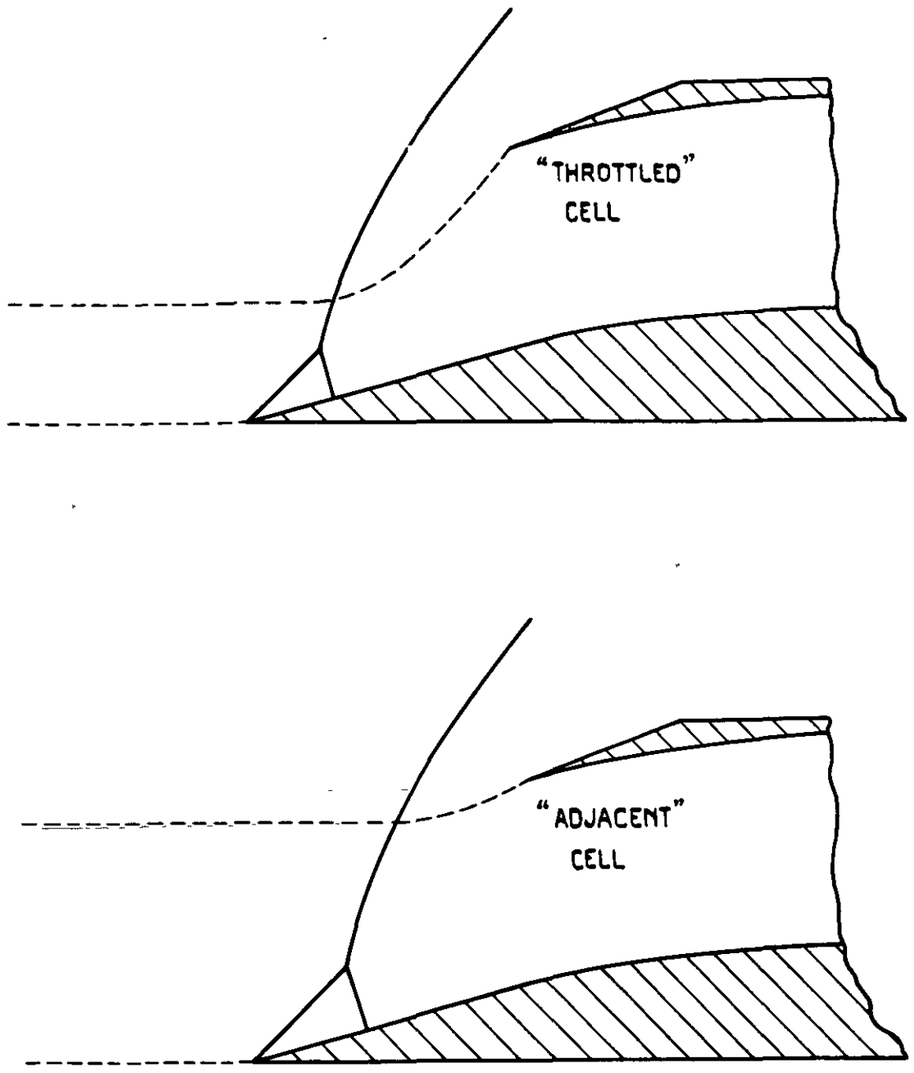

FIG. 21. SHOCK CONFIGURATIONS FOR CASE OF "ADJACENT" CELL HAVING LOWER MEAN PRESSURE RECOVERY THAN "THROTTLED" CELL.

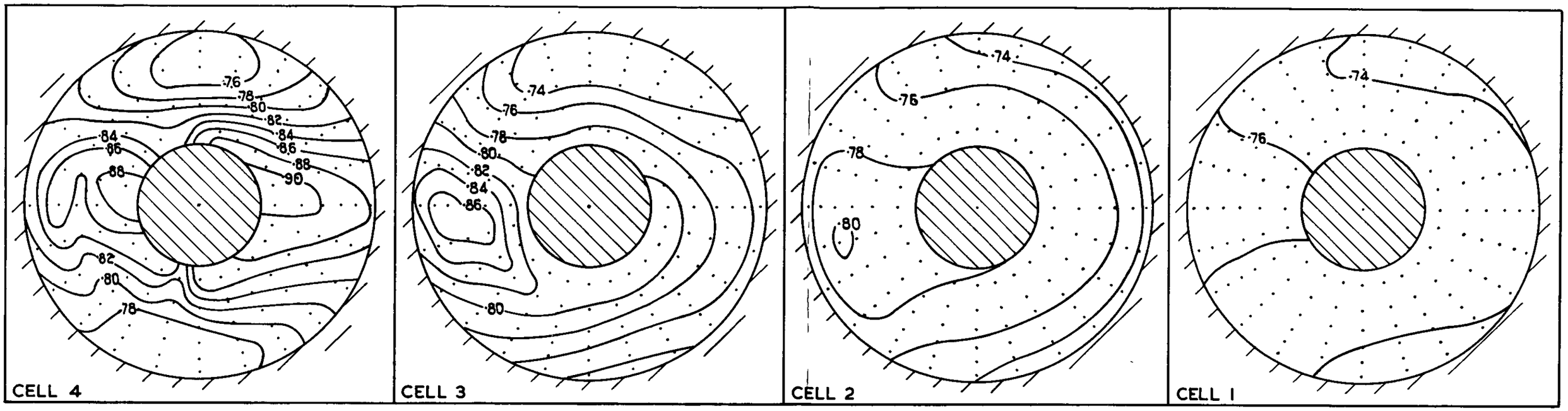

(a) CONFIGURATION A

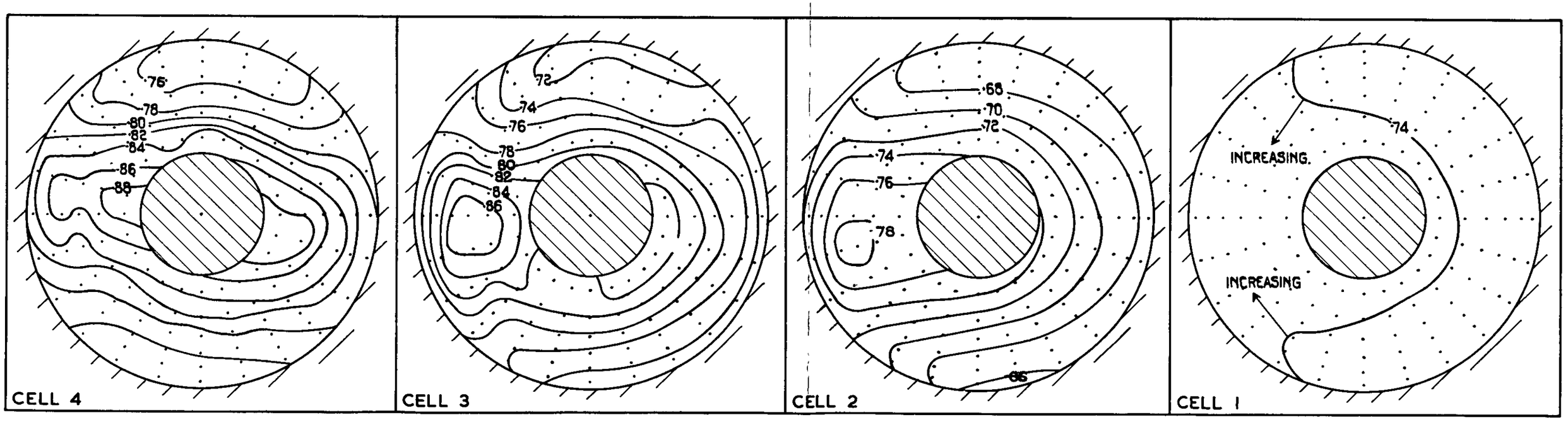

(b) CONFIGURATION B

FIG. 22. TOTAL PRESSURE DISTRIBUTIONS, LOOKING DOWNSTREAM, CELL 1 THROTTLED TO $A_{\infty}/A_{en} \doteq 0{\cdot}43$.

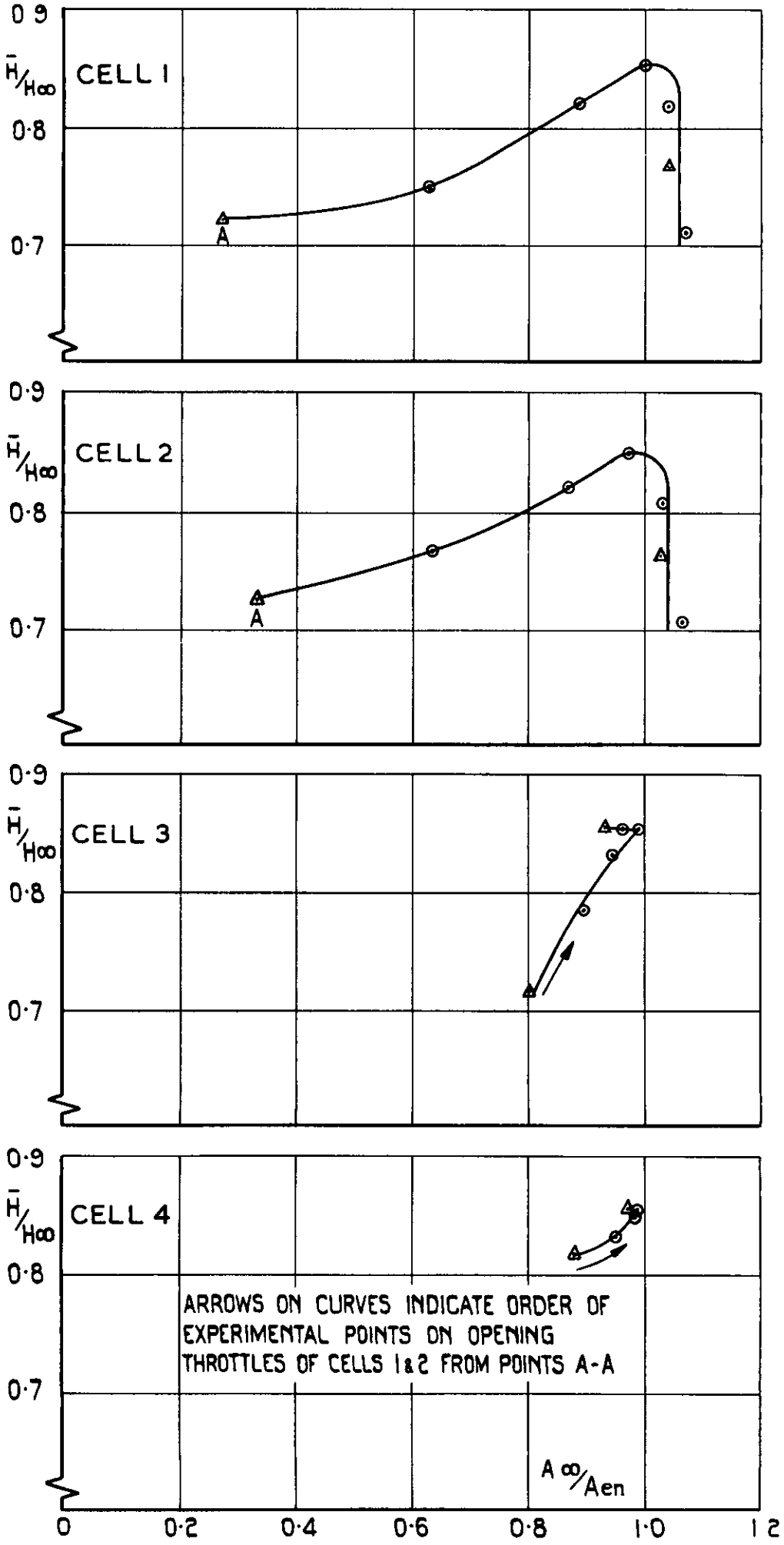

FIG.23. VARIATION OF PRESSURE RECOVERY WITH MASS FLOW RATIO, CONFIGURATION A, CELLS 1 & 2 THROTTLED.

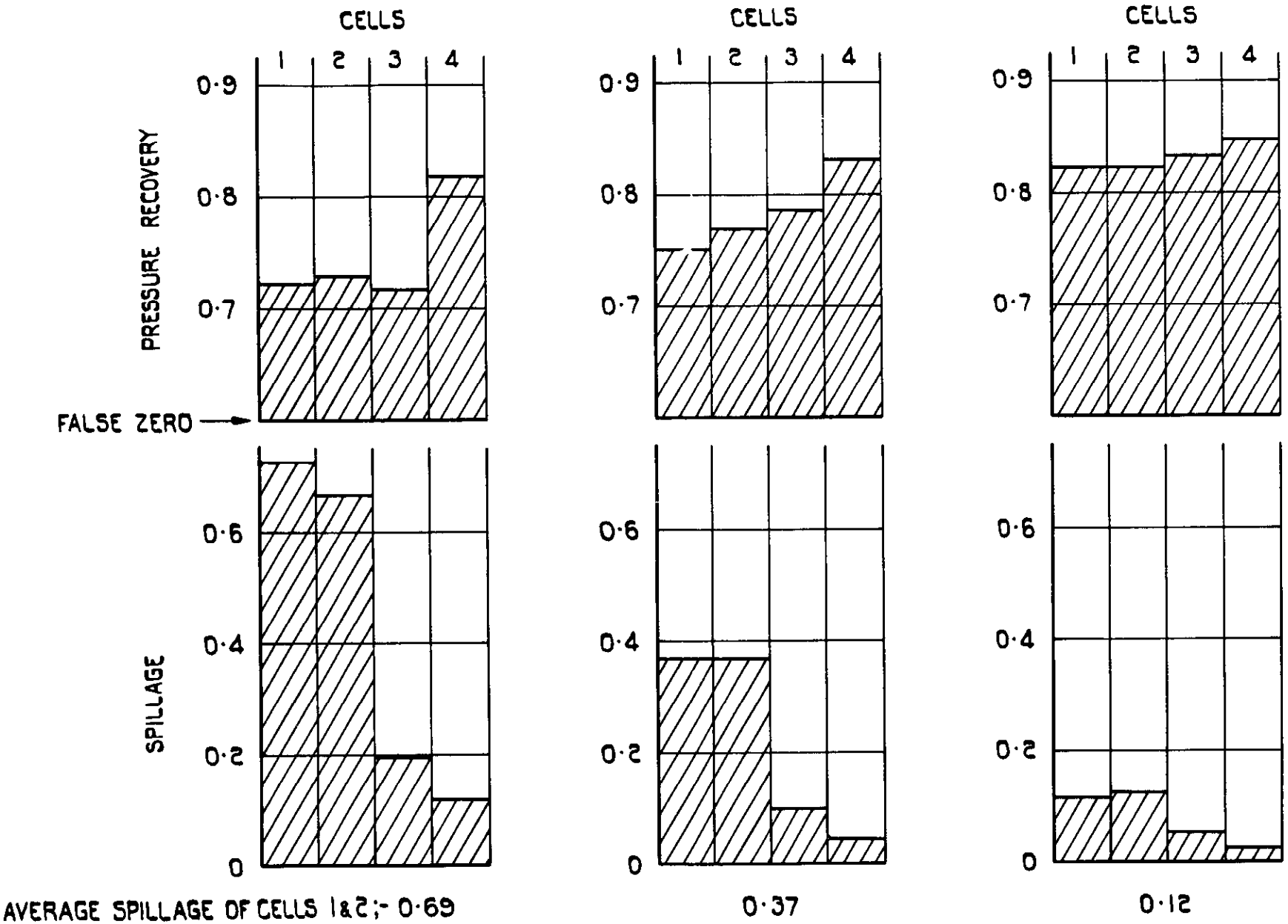

FIG. 24. BLOCK DIAGRAMS SHOWING PRESSURE RECOVERY & SPILLAGE IN CELLS WHEN CELLS 1&2 ARE THROTTLED, CONFIGURATION A.

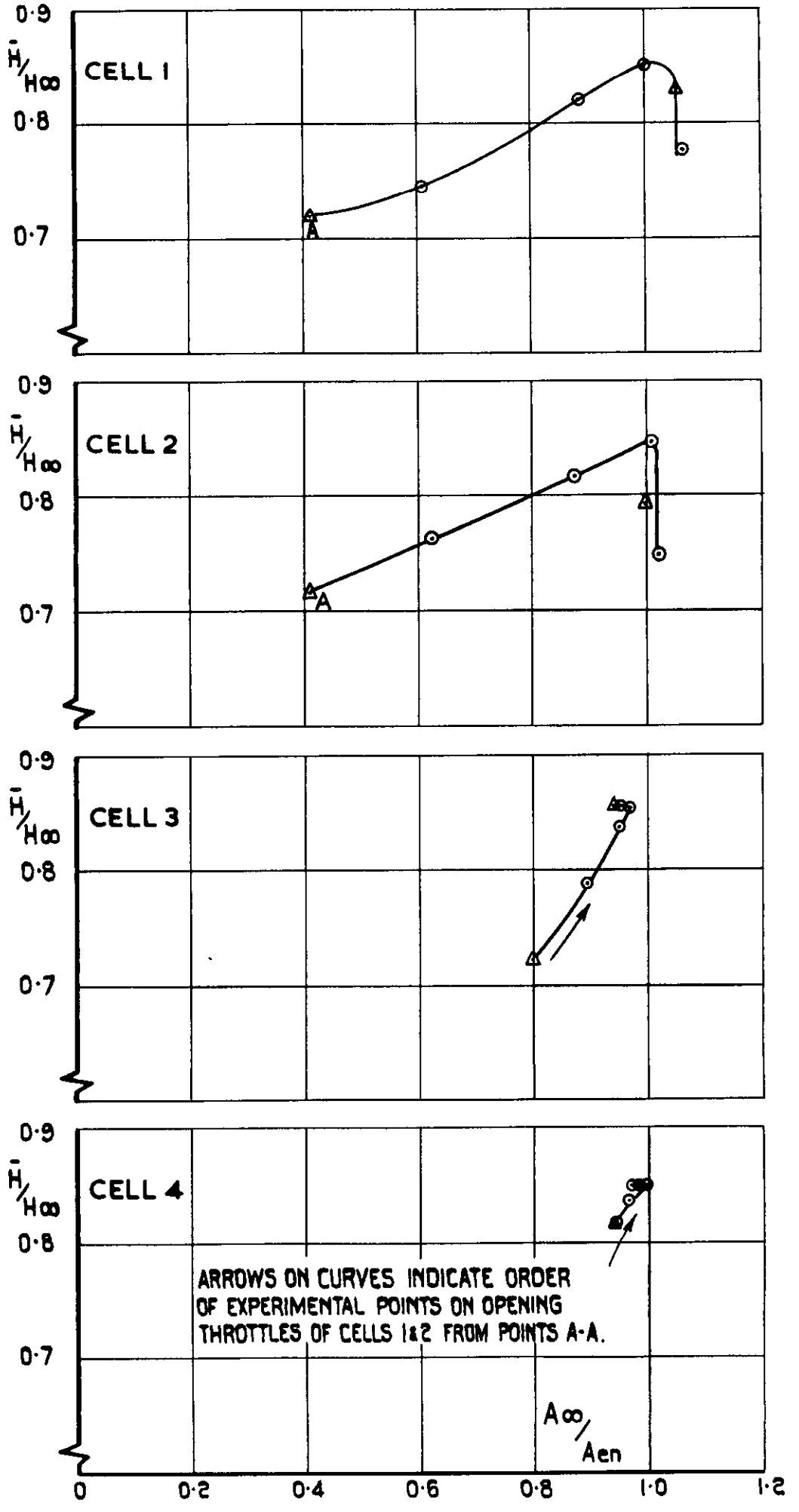

FIG.25. VARIATION OF PRESSURE RECOVERY WITH MASS FLOW RATIO, CONFIGURATION B, CELLS 1 & 2 THROTTLED.

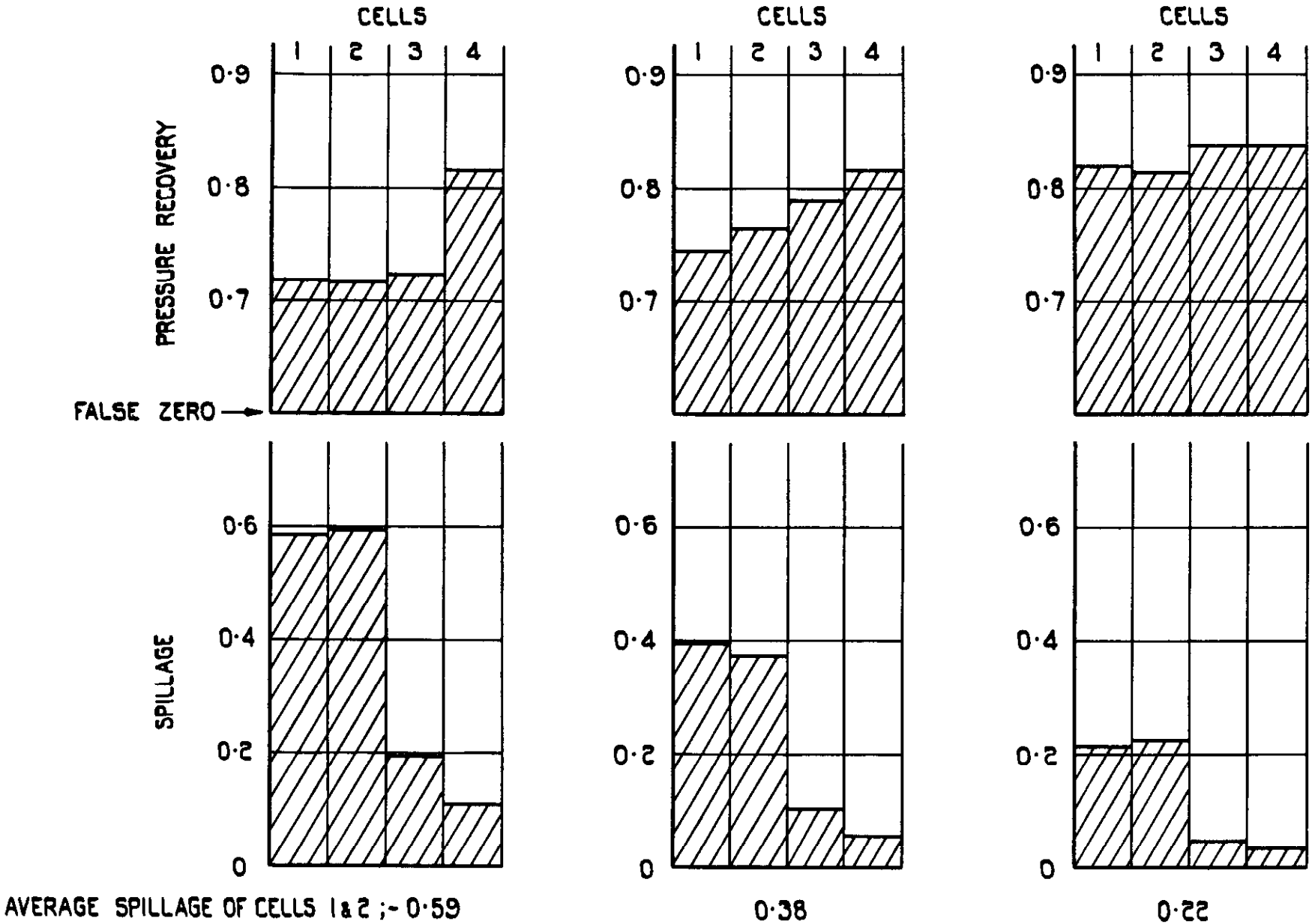

FIG.26. BLOCK DIAGRAMS SHOWING PRESSURE RECOVERY & SPILLAGE IN CELLS WHEN CELLS 1&2 ARE THROTTLED, CONFIGURATION B.

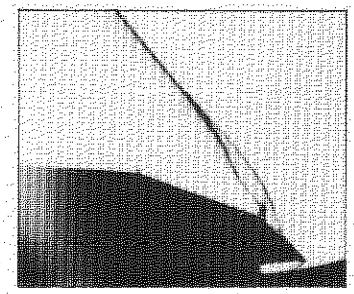

a. 0·87

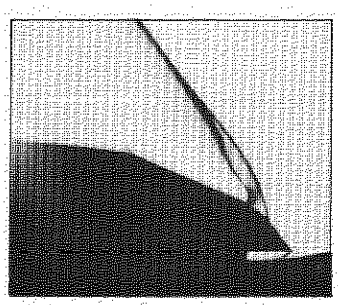

d. 0·88

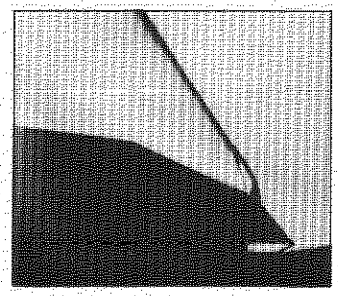

g. 0·91

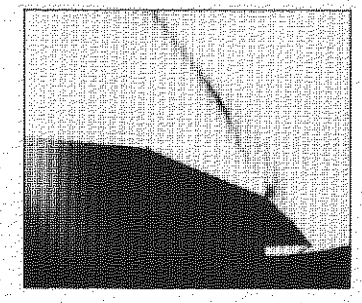

b. 0·85

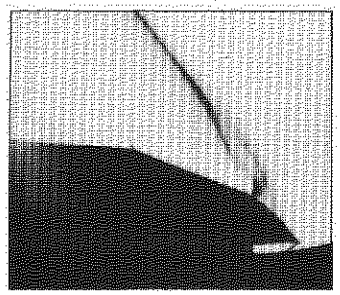

e. 0·84

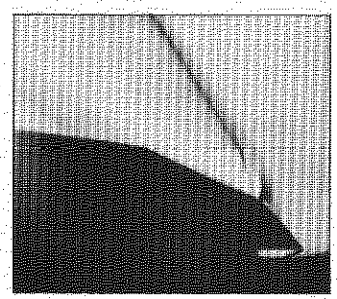

h. 0·85

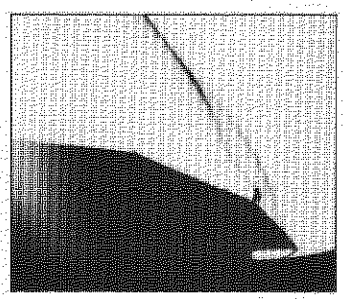

c. 0·83

CELL 1 THROTTLED

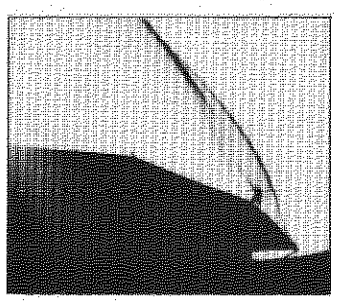

f. 0·81

CELLS 1 & 2 THROTTLED TOGETHER

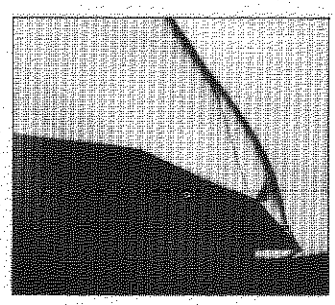

i. 0·72

ALL FOUR CELLS THROTTLED

THE NUMBER UNDER EACH PHOTOGRAPH IS THE APPROXIMATE MEAN OF THE MASS FLOW RATIOS THROUGH THE FOUR CELLS

FIG.27. SCHLIEREN PHOTOGRAPHS, SHOWING INTAKE INSTABILITY - CONFIGURATION A.

A.R.C. C.P. No. 753

533.697.2 :
533.6.011.5 :
533.695.9 :
621.438.018

WIND TUNNEL TESTS AT M = 2.0 ON INTERFERENCE EFFECTS BETWEEN INTAKE FLOWS IN A FOUR-ENGINE NACELLE. Dobson, M. D. September, 1963

A model of a rectangular air intake of aspect ratio 8, with all-external compression and a fixed geometry, has been tested at its design Mach number of 2.0 in the 3 ft x 3 ft wind tunnel. The model contained four side-by-side simulated engine cells and tests were made to investigate effects on pressure recovery and mass flow in each of the cells for conditions of unequal throttling.

Results showed that when the throttle of one cell was closed to give sub-critical inlet flow, the shock geometry at the inlet was affected and

(Over)

A.R.C. C.P. No. 753

533.697.2 :
533.6.011.5 :
533.695.9 :
621.438.018

WIND TUNNEL TESTS AT M = 2.0 ON INTERFERENCE EFFECTS BETWEEN INTAKE FLOWS IN A FOUR-ENGINE NACELLE. Dobson, M. D. September, 1963.

A model of a rectangular air intake of aspect ratio 8, with all-external compression and a fixed geometry, has been tested at its design Mach number of 2.0 in the 3 ft x 3 ft wind tunnel. The model contained four side-by-side simulated engine cells and tests were made to investigate effects on pressure recovery and mass flow in each of the cells for conditions of unequal throttling.

Results showed that when the throttle of one cell was closed to give sub-critical inlet flow, the shock geoemtry at the inlet was affected and

(Over)

A.R.C. C.P. No. 753

533.697.2 :
533.6.011.5 :
533.695.9 :
621.438.018

WIND TUNNEL TESTS AT M = 2.0 ON INTERFERENCE EFFECTS BETWEEN INTAKE FLOWS IN A FOUR-ENGINE NACELLE. Dobson, M. D. September, 1963.

A model of a rectangular air intake of aspect ratio 8, with all-external compression and a fixed geometry, has been tested at its design Mach number of 2.0 in the 3 ft x 3 ft wind tunnel. The model contained four side-by-side simulated engine cells and tests were made to investigate effects on pressure recovery and mass flow in each of the cells for conditions of unequal throttling.

Results showed that when the throttle of one cell was closed to give sub-critical inlet flow, the shock geometry at the inlet was affected and

(Over)

and pressure recovery and mass flow in the remaining cells were reduced. These reductions became progressively smaller in cells situated further from the throttle cell. Both pressure recovery and mass flow in a cell adjacent to one which was passing reduced flow ere affected also by the presence of duct dividers in the intake.

When the throttle of one cell was opened to give super-critical inlet flow, an adjacent cell was not affected if the duct was divided between the cells from the beginning of the subsonic diffuser. If the cells shared a common diffuser the adjacent cell suffered reductions in both pressure recovery and mass flow.

Schlieren observations indicate that the initial onset of instability under sub-critical flow conditions, occurs at the same mean mass flow ratio, irrespective of how the four throttles are individually set to achieve this ratio.

and pressure recovery and mass flow in the remaining cells were reduced. These reductions became progressively smaller in cells situated further from the throttle cell. Both pressure recovery and mass flow in a cell adjacent to one which was passing reduced flow were affected also by the presence of duct dividers in the intake.

When the throttle of one cell was opened to give super-critical inlet flow, and adjacent cell was not affected if the duct was divided between the cells from the beginning of the subsonic diffuser. If the cells shared a common diffuser the adjacent cell suffered reductions in both pressure recovery and mass flow.

Schlieren observations indicate that the initial onset of instability under sub-critical flow conditions, occurs at the same mean mass flow ratio, irrespective of how the four throttles are individually set to achieve this ratio.

Published by
HER MAJESTY'S STATIONERY OFFICE

To be purchased from
York House, Kingsway, London W C.2
423 Oxford Street, London W.1
13A Castle Street, Edinburgh 2
109 St Mary Street, Cardiff
39 King Street, Manchester 2
50 Fairfax Street, Bristol 1
35 Smallbrook, Ringway, Birmingham 5
80 Chichester Street, Belfast 1
or through any bookseller

S.O. CODE No. 23-9015-53